Bound states of nonlinear Schrödinger equations with a periodic nonlinear microstructure

G. Fibich [a], Y. Sivan [b], M.I. Weinstein [c]

[a] *School of Mathematical Sciences, Tel Aviv University, Tel Aviv, 69978 Israel*

[b] *School of Physics and Astronomy, Tel Aviv University, Tel Aviv, 69978 Israel*

[c] *Department of Applied Physics and Applied Mathematics, Columbia University, New York, NY 10027*

Contents

Abstract

We consider nonlinear bound states of the nonlinear Schrödinger equation

$$i\partial_z\phi(z,x) = -\partial_x^2\phi - (1 + m(Nx))|\phi|^{p-1}\phi,$$

in the presence of a nonlinear periodic microstructure $m(Nx)$. This equation models the propagation of laser beams in a medium whose nonlinear refractive index is modulated in the transverse direction, and also arises in the study of Bose-Einstein Condensation (BEC) in a medium with a spatially dependent scattering length. In the nonlinear optics context, $N = r_{\text{beam}}/r_{\text{ms}}$ denotes the ratio of beam width to microstructure characteristic scale. We study the profiles of the nonlinear bound states using a multiple scale (homogenization) expansion for $N \gg 1$ (wide beams), a perturbation analysis for $N \ll 1$ (narrow beams) and numerical simulations for $N = \mathcal{O}(1)$. In the subcritical case $p < 5$, beams centered at local maxima of the microstructure are stable. Furthermore, beams centered at local minima of the microstructure are unstable to general (asymmetric) perturbations but stable relative to symmetric perturbations. In the critical case $p = 5$, a nonlinear microstructure can only stabilize narrow beams centered at a local maximum of the microstructure, provided that the microstructure also satisfies a certain local condition. Even in this case, the stability region is very small so that small ($\mathcal{O}(10^{-2})$) perturbations can destabilize the beam. Therefore, such beams are "mathematically" stable but "physically" unstable.

Key words: Microstructure, Homogenization, Instability, Collapse, Periodic potential, Solitary waves, Nonlinear waves, Bose-Einstein Condensation (BEC).
PACS: 42.65.Tg, 42.65.Jx, 03.75.Lm

1 Introduction and overview

The propagation of linearly-polarized, paraxial laser beams in a *homogeneous* Kerr medium can be modeled by the nonlinear Schrödinger equation (NLS)

$$i\partial_z\phi(z,\mathbf{x}) = -\Delta\phi - |\phi|^2\phi, \qquad \phi(0,\mathbf{x}) = \phi_0(\mathbf{x}). \tag{1.1}$$

Here ϕ is the slowly-varying envelope of the electric field, z measures the distance in the direction of propagation, $\mathbf{x} = (x_1, ..., x_d)$ is the d-dimensional transverse vector and $\Delta = \partial_{x_1}^2 + \cdots + \partial_{x_d}^2$ is the $d-$dimensional Laplacian (diffraction) operator. The case $d = 1$ corresponds to propagation of beams in

Email addresses: fibich@tau.ac.il (G. Fibich), yonatans@post.tau.ac.il (Y. Sivan), miw2103@columbia.edu (M.I. Weinstein).

a planar geometry (slab waveguide), $d = 2$ to propagation in a bulk medium, and $d = 3$ to propagation of pulses in a bulk medium with anomalous time dispersion (in this case, time plays the role of a third "spatial" variable). The cubic (Kerr) nonlinearity in (1.1) results from the dependence of the refractive index on the electric field intensity

$$n = n_0 + n_2|\phi|^2, \tag{1.2}$$

where n_0 and n_2 are constants that denote the linear and nonlinear refractive indices of the medium, respectively.

The NLS
$$i\partial_t\psi(t, \mathbf{x}) = -\Delta\psi - |\psi|^2\psi,$$
also models the dynamics of Bose-Einstein Condensates (BEC), which are the subject of numerous recent theoretical and experimental investigations. In that context, the NLS is also known as the Gross-Pitaevskii (GP) equation. In this equation, typically $\mathbf{x} = (x, y, z)$, i.e., $d = 3$, but the cases $d = 1$ and $d = 2$ are also of physical interest.

In order to understand the relative effects of diffraction $(-\Delta)$ and nonlinearity $(|\psi|^2)$ in Eq. (1.1), it is useful to consider the more general NLS

$$i\partial_z\phi = -\Delta\phi - |\phi|^{p-1}\phi, \tag{1.3}$$

with a nonlinearity exponent $p > 1$. We delineate several cases for the NLS (1.3):

$$
\begin{aligned}
p &< 1 + \frac{4}{d}, &&\text{the subcritical case,} \\
p &= 1 + \frac{4}{d}, &&\text{the critical case,} \\
p &> 1 + \frac{4}{d}, &&\text{the supercritical case.}
\end{aligned}
\tag{1.4}
$$

In the subcritical case we have global existence in z, *i.e.* arbitrary H^1 initial conditions give rise to solutions which exist for all z. In contrast, in the critical and supercritical cases NLS solutions can become singular after propagating a finite distance Z_c. The critical case is characterized by a sharp L^2 norm (power) threshold $\mathcal{P}_{cr}(d)$, such that for $\mathcal{P} \geq \mathcal{P}_{cr}$ singularity formation can occur, while for $\mathcal{P} < \mathcal{P}_{cr}$ solutions diffract to zero with advancing z, where $\mathcal{P} = \int |\phi_0|^2 d\mathbf{x}$ is the beam power [1] [54,55]. The critical case $p = 1 + 4/d$ is distinguished by the property that in this case the power, $\mathcal{P}$, is invariant under the natural dilation scaling of NLS (1.3), $\phi(\cdot, \mathbf{x}) \mapsto \phi_\lambda(\cdot, \mathbf{x}) \equiv \lambda^{2/(p-1)}\phi(\cdot, \lambda\mathbf{x})$, *i.e.* $\mathcal{P}[\phi_\lambda] = \mathcal{P}[\phi]$. For more information on NLS theory, see [50,52,54].

---

[1] We call the L^2 norm the power, since in the nonlinear optics context it corresponds to physical beam power.

The NLS (1.3) is derived from Maxwell's equations and the constituitive law (1.2) for a *homogeneous* Kerr nonlinear medium. Recent advances in fabrication methods now make possible the fabrication of transparent media with rapidly varying, high contrast refractive properties (see *e.g.* [31,32]) with potential light-processing applications ranging from optical communication transmission media to quantum information science. Thus there is considerable interest in understanding the propagation of light in microstructure media.

Linear microstructures: Most studies have considered *linear microstructures*, *i.e.*, those for which n_0 is modulated while n_2 remains uniform. Nonlinear bound states (stationary self-trapped beams) in the presence of a *periodic linear microstructure* in the direction of propagation, i.e.,

$$n = n_0(z) + n_2|\phi|^2,$$

have been studied both analytically and experimentally; see, e.g., the review [7] and references therein. Such a microstructure can support propagation of *gap solitons* [17,36] and gives rise to phenomena such as *slow light* [15]. Trapping of gap soliton pulses in periodic structures with localized defects has been studied in [26,27]. This has potential applications to optical buffering, high-density storage and optical gates. Propagation of light in media with a linear microstructure where n_0 is modulated in the transverse plane, i.e.,

$$n = n_0(\mathbf{x}) + n_2|\phi|^2$$

was studied in [24,42,46]. Other studies considered transverse *periodical linear microstructures*, also known as *photonic lattices*. In particular, the limiting regimes of the discrete ("tight binding") and semi-discrete NLS can be used to demonstrate the existence and stability of *discrete solitons* [3,4,8,14,19,58,59]. In the context of quantum mechanics [23] there is the related notion of quantum breathers. Further studies used the continuous NLS model to study *lattice solitons* and their relation to the detailed band-gap structure [22,41,51]. **For a recent review, see [9] and references therein.**

In certain studies of BECs, condensates are studied in the background of periodic linear medium ($n_0(\mathbf{x})$ or equivalently $V(x)$ in the NLS / GP equation) or *optical lattice*, induced by the interference of laser beams. As a result, dynamics of condensates loaded on *optical lattices* are similar to the dynamics of discrete solitons [13,49] or lattice solitons [18]. For a review of these BEC studies, see [?,?].

Nonlinear microstructures: Recent success in the fabrication of media with a rapidly varying *nonlinear* refractive index [31] have motivated the study of

NLS with a spatially varying nonlinear coefficient, i.e., a *nonlinear microstructure*. This corresponds to media where n_2 is modulated and n_0 is constant. **In the BEC context, the analogous situation is one where the scattering length (controlled by the Feshbach resonance) varies in space. The possibility of controlling the scattering length [20,53] makes it possible to induce a spatially and temporally dependent nonlinearity.** The case of a periodic nonlinearity in the direction of propagation, i.e.,

$$n = n_0 + n_2(z)|\phi|^2,$$

was analyzed in [1,12,43,47] in the context of a nonlinear analog of dispersion management, sometimes called *nonlinearity management* **and in [1,39] in the context of BEC.**

The case considered in this paper, of modulation of n_2 in the transverse direction, *i.e.*,

$$n = n_0 + n_2(\mathbf{x})|\phi|^2, \tag{1.5}$$

has received little attention thus far. Merle [37,38] studied the properties of blowup solutions of

$$i\partial_z\phi \ = \ -\Delta\phi - g(\mathbf{x})|\phi|^{p-1}\phi, \tag{1.6}$$

in the critical case $p = 1 + 4/d$. Fibich and Wang found a condition for the stability of radially-symmetric, narrow bound states of Eq. (1.6) in the critical case [21]. **Studies of Eq. (1.6) in the context of BEC were done mainly for the case $d = 1$ and $p = 3$ (subcritical case) using the moment method and standard soliton perturbation techniques [?,1,48,53]. In [?], results of soliton motion and radiation were obtained. In [?], specific conditions for stability were derived for the subcritical case when $d \geq 3$. Finally, Hajaiej and Stuart [30] proved the stability of the constrained energy minimizers (ground states) of Eq. (1.6) in the *d-dimensional* subcritical case.**

In this paper we consider Eq. (1.6) in one transverse dimension x, which corresponds to propagation in a planar geometry ($d = 1$). Hence, $p < 5$ corresponds to subcritical self-focusing, and $p = 5$ to critical self-focusing. Since both cases, $(d, p) = (1, 5)$ and $(d, p) = (2, 3)$ are critical, the case $p = 5$ with one transverse dimension is mathematically analogous to the physical case of Kerr (cubic) nonlinearity $p = 3$ in two transverse dimensions (i.e., propagation in a bulk Kerr medium) [?].

We focus on the case of a *periodic* nonlinear microstructure in the transverse direction, corresponding to the design of many manufactured slab microstructure waveguides. In this case, the propagation is governed by the one-dimensional NLS

$$i\partial_z\phi = \ -\partial_x^2\phi \ - \ (1 + m(Nx))|\phi|^{p-1}\phi, \tag{1.7}$$

6

where the periodic function $m(Nx)$ describes the nonlinear microstructure variations in the transverse direction (see Fig. 1).

The paper is organized as follows. In Section 2, we derive Eq. (1.7) from the Helmholtz equation with a nonlinear microstructure refractive index. In this derivation it is useful to introduce the parameter N, which measures the ratio of the input beam width r_{beam} to the microstructure period r_{ms},

$$N = \frac{r_{beam}}{r_{ms}}. \tag{1.8}$$

Thus, $N \ll 1$ corresponds to *narrow beams* (beams which are narrower than the microstructure period) and $N \gg 1$ corresponds to *wide beams* (beams which are wider than the microstructure period). We find that the stability properties of microstructure bound states are strongly dependent on N.
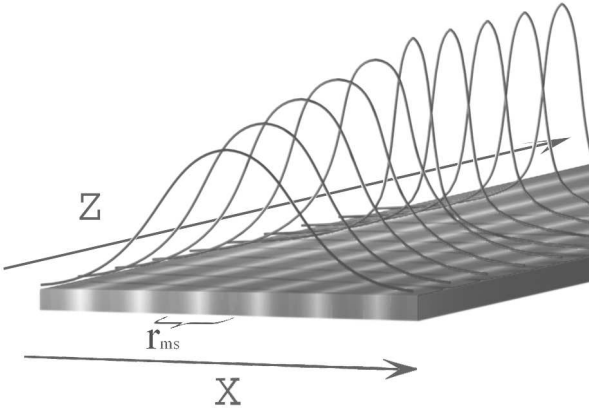

Fig. 1. Graphical illustration of a medium with a microstructure in the transverse plane.

Bound states $\phi = e^{i\nu z} u^{(N)}(x; \nu)$ of Eq. (1.7) satisfy the equation

$$-\partial_x^2 u^{(N)} - (1 + m(Nx)) \left(u^{(N)}\right)^p + \nu u^{(N)} = 0. \tag{1.9}$$

In Section 3.1, we solve this equation in the case of wide ($N \gg 1$) bound states using a *multiple scale expansion* (Theorem 3). The expansion shows that, to leading order in $1/N$, $u^{(N)}$ is a nonlinear bound state of a homogeneous medium with an *average* Kerr nonlinearity coefficient $\langle n_2 \rangle$. Here, $\langle n_2 \rangle$ is equal to the arithmetic average of $n_2(x)$ over one microstructure period. Corrections due to microstructure in the nonlinear bound state profile arise only at $\mathcal{O}(N^{-2})$. Therefore, even when the microstructure variations are $\mathcal{O}(1)$, the microstructure has a small effect on the bound state profile. We also prove that nonlinear microstructure always reduces the L^2 norm (power) of wide bound states (Theorem 7). **Since our multiple scales expansion remains valid for high-contrast microstructure and even for $\max_x |m(Nx)| > 1$, our**

analysis covers situations where the nonlinearity coefficient changes sign.

We note that standard homogenization theory [11] can also be used in order to calculate the leading order solution of Eq. (1.9). However, for $N \gg 1$, computation of the $\mathcal{O}(N^{-2})$ correction due to microstructure is essential in the case of critical nonlinearities ($p = 5$) since for $N = \infty$ the solitary wave is only marginally unstable (algebraic growth of the linearized evolution). Our study of the first non-trivial corrections in $1/N$ shows that the highly degenerate (due to criticality) zero mode of the linearized operator perturbs to an exponential instability, a result which cannot be obtained by leading order homogenization. Two other problems where homogenization gives an an incomplete picture are [25,35].

In Section 3.2, we use perturbation analysis to obtain an expansion in powers of N for narrow bound states ($N \ll 1$). As in the case of wide beams, the leading order term in the expansion is a nonlinear bound state of the homogeneous NLS. Here, the uniform Kerr coefficient is determined by the *local* properties of the microstructure. As in the case of wide beams, even when the microstructure variations are not small, the microstructure has a small effect on the bound state profile. We also show that the microstructure leads to an $\mathcal{O}(N^2)$ change in the bound state power for $p \neq 5$, but only an $\mathcal{O}(N^4)$ change in the critical case $p = 5$.

With asymptotic expansions of nonlinear bound states in hand, in Section 4 we turn to the question of the dynamical stability of the waveguide solutions $\phi_{wg}(x, z) = u^{(N)}(x; \nu)e^{i\nu z}$. General conditions for stability and instability for equations of nonlinear Schrödinger equations were given in [29,56,57]. These conditions, which ensure that the bound state, which is a critical point of an appropriate energy functional, is in fact a local minimizer, are as follows (see Theorem 10):

(S1) The linearized operator

$$L_+^{(N)} \equiv -\partial_x^2 + \nu + p\,(\, 1 + m(Nx)) \left(u^{(N)}(x) \,\right)^p$$

has no more than one negative eigenvalue (*spectral condition*).

(S2) $\partial_\nu \, \|u^{(N)}(x; \nu)\|_2^2 > 0$ (*slope condition*).

We apply these two conditions to study the stability and instability of wide ($N \gg 1$), $\mathcal{O}(1)$ and narrow ($N \ll 1$) beams for subcritical ($p < 5$) and critical ($p = 5$) cases. In the subcritical case, beams centered at a local maximum of the microstructure are stable while beams centered at a local minimum of the microstructure are stable relative to symmetric perturbations (*symmetric problem*) but unstable under general, symmetry-breaking perturbations (*gen-*

	Symmetric problem		General problem	
	local maximum	local minimum	local maximum	local minimum
$N \gg 1$	*stable*	*stable*	*stable*	probably [a] unstable
$N = \mathcal{O}(1)$	*stable*	*stable*	*stable*	unstable
$N \ll 1$	*stable*	*stable*	*stable*	unstable

Table 1
Stability of beams with various widths for the subcritical case $p = 3$. Since the power slope is always positive, stability is determined by the number of negative eigenvalues.

[a] See discussion in Section 4.6.1.

	Symmetric problem		General problem	
	local maximum	local minimum	local maximum	local minimum
$N \gg 1$	unstable*	unstable*	unstable*	unstable*
$N = \mathcal{O}(1)$	unstable*	*stable*	unstable*	unstable[†]
$N \ll 1$	determined by Eq. (4.14)		determined by Eq. (4.14)	unstable[†]

Table 2
Stability of beams with various widths for the critical case $p = 5$. Source for instability is marked by * for a negative slope and by [†] for a second negative eigenvalue.

eral problem), see Table 1. In the critical case, only narrow beams centered at a local maximum of a microstructure that satisfies condition (4.14) can be stable, while wide and $\mathcal{O}(1)$ beams centered at a local maximum are unstable due to a negative slope. Beams centered at a local minimum are unstable due to a second negative eigenvalue (violation of (S1)); see Table 2.

An interesting case is that of $\mathcal{O}(1)$ beams centered at a local minimum. Although the slope condition (S2) holds both for the subcritical and critical cases, the beam is still seen to be unstable. Indeed, the linearized operator $L_+^{(N)}$ has two negative eigenvalues, the larger of which corresponds to a asymmetric eigenstate. Instability then follows from Theorem 10. Insight into the nature of this instability can be obtained by an Ehrenfest-type calculation: we show in Section 4.7 that the acceleration of the *center of mass* of the beam is always in the direction of the nearest local maximum of the microstructure. In other words, the instability of beams centered at a local minimum of the microstructure is due to the tendency of the beam to move toward regions of higher nonlinear index of refraction. This *drift instability* is related to an excitation of the asymmetric second mode of $L_+^{(N)}$. Due to the reflection symmetry of the equation about local minima, stability can be restored by constraining

9

to initial data which are *symmetric* about the local minimum.

In Section 4.5, we show that in the case of $\mathcal{O}(1)$ beams the definition of a beam "centered" at a microstructure maximum or minimum is more subtle. This is due to the fact that, unlike narrow beams, an $\mathcal{O}(1)$ beam interacts with a more extended spatial "landscape". Therefore, in order to determine the stability properties of an $\mathcal{O}(1)$ beam, one needs to average out microstructure changes which are more rapid than the $\mathcal{O}(1)$ beam scale. We observe that a coarse-grained description, in terms of a locally averaged but not globally averaged description, may be most appropriate for defining whether the beam is centered at a microstructure maximum or minimum.

In Section 5 we illustrate the stability and instability results of Section 4 through numerical simulations. In the subcritical case $p = 3$ (Section 5.1), bound states centered at a local maximum of the microstructure are indeed stable, as well as beams centered at a local minimum of the microstructure that are perturbed by a symmetric perturbation. However, asymmetric perturbations (e.g., a lateral shift of the beam center) causes beams centered at a local minimum to drift toward the nearest local maximum and to oscillate about it. As noted earlier, this *drift instability* is related to the existence of a second (asymmetric) negative eigenvalue. In the critical case $p = 5$ (Section 5.2), our simulations show that whenever the instability originates from a failure to satisfy the slope condition (e.g., wide and $\mathcal{O}(1)$ beams centered at a microstructure maximum), the beam undergoes either blowup or total diffraction, depending on its initial power. This *blowup/diffraction instability* is similar to the case of homogeneous NLS. As in the subcritical case, whenever the instability originates from a second negative eigenvalue (i.e., beams centered at a local minimum), the solution exhibits a *drift instability*. However, unlike the subcritical case, these beams blowup as they drift rather than oscillate about the microstructure maximum. Depending on the input beam power, the blowup point can be before or after the nearest local maximum. Finally, we confirm that narrow beams centered at a local maximum of a microstructure that satisfies condition (4.14) are stable. We expect, however, that this stability is more of mathematical than physical interest since the magnitude of the positive slope is only $\mathcal{O}(N^4)$ small. Indeed, we find that the beam is stable under perturbations of size $\mathcal{O}(10^{-4})$ but becomes unstable under perturbations of order $(\mathcal{O}(10^{-2}))$. Section 6 contains a summary and concluding discussion.

2 Theory of stationary beams in nonlinear microstructures

2.1 Derivation of NLS

Consider the scalar nonlinear Helmholtz equation

$$\Delta E(z, x) + \frac{\omega_0^2}{c^2} n^2(x, |E|^2) E = 0, \tag{2.1}$$

as a model for the propagation of linearly-polarized, monochromatic beams in a planar waveguide with a Kerr-type nonlinearity. Here E denotes the electric field, z the direction of propagation, x the transverse coordinate, $\Delta = \partial_z^2 + \partial_x^2$, ω_0 the carrier frequency, c the speed of light in vacuum and n the refractive index. In this paper we analyze the case where the linear index of refraction n_0 is uniform, but the nonlinear index of refraction n_2 is periodically modulated in the transverse direction x, i.e.,

$$n(x) = n_0 + n_2(x)|E|^2, \quad n_2(x) = \bar{n}_2 + \delta n_2\left(\frac{x}{r_{ms}}\right), \tag{2.2}$$

where n_0 and $\bar{n}_2$ are constants and $\delta n_2(\frac{x}{r_{ms}})$ is periodic with period r_{ms}. We introduce the standard non-dimensional variables

$$\tilde{z} \equiv \frac{z}{2k_0 r_{beam}^2}, \quad \tilde{x} \equiv \frac{x}{r_{beam}}, \quad E = e^{ik_0 z}(2n_0 \bar{n}_2 k_0^2 r_{beam}^2)^{-\frac{1}{2}} \phi, \tag{2.3}$$

where $k_0 = \omega_0 n_0 / c$ denotes the wavenumber in the medium and r_{beam} the width of the incident beam. Substituting the rescaling (2.3) in Eq. (2.1), assuming the Kerr nonlinearity is small (i.e., $n_2|\phi|^2 \ll n_0$) and using the paraxial approximation ($\phi_{zz} \ll k_0 \phi_z$) we obtain for $\phi(\tilde{z}, \tilde{x})$:

$$i\partial_{\tilde{z}}\phi = -\partial_{\tilde{x}}^2 \phi - (1 + m(N\tilde{x}))|\phi|^2 \phi,$$

where $m(N\tilde{x}) = \delta n_2(N\tilde{x})/\bar{n}_2$ and

$$N \equiv r_{beam}/r_{ms}.$$

Therefore, $N \gg 1$ describes the situation of a wide input beam ($r_{beam} \gg r_{ms}$) and $N \ll 1$ describes a narrow beam ($r_{ms} \gg r_{beam}$); but see also Remark 2 below.

In what follows, we consider a more general equation with a general power nonlinearity $p > 1$, rather than only the cubic case ($p = 3$). Thus, suppressing the tildes, we get

$$i\partial_z\phi = -\partial_x^2 \phi - (1 + m(Nx))|\phi|^{p-1}\phi, \quad \phi(0, x) = \phi_0(x). \tag{2.4}$$

When the nonlinear index of refraction is also uniform, i.e., $\delta n_2(Nx) \equiv 0$, then $m \equiv 0$ and Eq. (2.4) reduces to the homogeneous nonlinear Schrödinger equation

$$i\partial_z \phi = -\partial_x^2 \phi - |\phi|^{p-1}\phi. \tag{2.5}$$

The natural scaling of the spatial variable of the microstructure variations is $X \equiv Nx$. Indeed, under this definition, $m = m(X)$ is periodic with period 1.

Remark 1 *Without loss of generality, we can assume that the $X-$ average of m is zero, i.e.,*

$$\langle m \rangle \equiv \int_0^1 m(X) \, dX = 0. \tag{2.6}$$

Indeed, if the average of m is nonzero, we can define $m \equiv \tilde{m} + \langle m \rangle$ and $\tilde{\phi} = \phi / (1 + \langle m \rangle)^{\frac{1}{p-1}}$ so that $\tilde{\phi}$ satisfies Eq. (2.4) with a mean-zero periodic nonlinear microstructure.

We also assume that m is an even function. Thus, m satisfies the following three requirements:

$$\langle m \rangle = 0, \quad m(X) = m(-X), \quad m(X) = m(X+1). \tag{2.7}$$

2.2 Bound states

We seek nonlinear bound states of Eq. (2.4) of the form

$$\phi(z, x) = e^{i\nu z} u^{(N)}(x; \nu),$$

where $u^{(N)}$ is a real function. The equation for $u^{(N)}$ becomes

$$\frac{d^2}{dx^2} u^{(N)} + (1 + m(Nx))(u^{(N)})^p - \nu u^{(N)} = 0, \quad u^{(N)}(\pm\infty) = 0. \tag{2.8}$$

Recall that in a homogeneous medium ($m \equiv 0$), Eq. (2.8) reduces to

$$\frac{d^2}{dx^2}\mathcal{U} + \mathcal{U}^p - \nu\,\mathcal{U} = 0, \tag{2.9}$$

whose solution is given by

$$\mathcal{U}(x, \nu) = \left(\frac{p+1}{2}\nu\right)^{\frac{1}{p-1}} \operatorname{sech}^{\frac{2}{p-1}}\left(\frac{p-1}{2}\sqrt{\nu}x\right). \tag{2.10}$$

Since the nonlinear microstructure is symmetric with respect to $x = 0$, in what follows we will look for bound states that are also symmetric with respect to $x = 0$. Therefore, we can replace Eq. (2.8) with the following boundary value

problem on the positive real line:

$$\frac{d^2}{dx^2}u^{(N)} + (1 + m(Nx))(u^{(N)})^p - \nu\, u^{(N)} = 0, \quad d_x u^{(N)}(0) = 0, \quad u^{(N)}(\infty) = 0,$$

(2.11)

for $0 < x < \infty$. The solution on all $\mathbb{R}$ is obtained by reflection about $x = 0$.

Remark 2 *Under the transformation $u^{(\tilde{N})} = \nu^{\frac{1}{p-1}}\, u^{(N)}(\sqrt{\nu}x)$, Eq. (2.11) becomes*

$$-\frac{d^2}{dx^2}u^{(\tilde{N})} - (1 + m(\tilde{N}x))(u^{(\tilde{N})})^p + u^{(\tilde{N})} = 0, \quad \tilde{N} \equiv \frac{N}{\sqrt{\nu}}.$$

(2.12)

Therefore, the parameter that determines whether the bound state of (2.11) is wide or narrow is $\tilde{N}$ rather than N. However, since the width of the bound state is $\approx \nu^{-\frac{1}{2}}$ (see Eq. 2.10) and since the rescaling (2.3) implies that the nondimensional width is $\mathcal{O}(1)$, if follows that $\nu = \mathcal{O}(1)$ in Eq. (2.11).

3 Calculation of bound states

3.1 Calculation of wide bound states $(N \gg 1)$ using multiple scales analysis

We now adopt a multiple scale approach to calculate an asymptotic approximation of wide bound states $(N \gg 1)$, i.e., bound states whose width is at least a few microstructure periods long $(r_{beam} \gg r_{ms})$:

Theorem 3 *Let $m(X)$ satisfy Eq. (2.7) and let $N \gg 1$. Then, the solution of Eq. (2.11) is given by*

$$u^{(N)}(x; \nu) = \mathcal{U}(x, \nu) - \frac{1}{N^2}\left(\mathcal{U}^p\, [\partial_X^{-2}m(X)] - p\tau_m L_+^{-1}[\mathcal{U}^{2p-1}]\right)$$
$$+ \mathcal{O}(N^{-4}),$$

(3.1)

where $\mathcal{U}$ is given by Eq. (2.10), $X = Nx$, ∂_X^{-2} is given by (3.15) with $k = 2$,

$$\tau_m = -\langle m\, \partial_X^{-2}m \rangle = \langle [\partial_X^{-1}m]^2 \rangle > 0,$$

(3.2)

the average $\langle \cdot \rangle$ is given by Eq. (2.6), and

$$L_+ = -d_x^2 + \nu - p\mathcal{U}^{p-1}(x, \nu).$$

(3.3)

Since $\lim_{N\to\infty} u^{(N)} = \mathcal{U}$, Theorem 3 shows that as $N \to \infty$ the bound state only "feels" the average nonlinear refractive index $\bar{n}_2 = \frac{1}{r_{ms}}\int_x^{x+r_{ms}} n_2(x)\, dx$;

13

see (2.2). At large but finite values of N, wide bound states differ from the bulk bound state only by an $\mathcal{O}(N^{-2})$ term. Note that this holds even when m undergoes $\mathcal{O}(1)$ changes, i.e., when δn_2 is comparable in magnitude to $\bar{n}_2$ (see, e.g., Fig. 7).

Proof: We view the solution $u^{(N)}$ as a function of a slow scale x and a fast scale $X = Nx$, i.e., $u^{(N)} = u^{(N)}(x, X)$. In terms of the independent variables x and X, d/dx is replaced by $\partial_x + N\partial_X$ so that Eq. (2.11) can be rewritten as

$$-\left(\partial_x^2 + 2N\partial_x\partial_X + N^2\partial_X^2\right) u^{(N)}(x, X) - (1 + m(X))\left(u^{(N)}\right)^p + \nu u^{(N)} = 0. \tag{3.4}$$

We expand the solution of (3.4) in a power series in N^{-1}, i.e.,

$$u^{(N)}(x, X) = u_0(x, X) + \frac{1}{N}u_1(x, X) + \frac{1}{N^2}u_2(x, X) + \cdots. \tag{3.5}$$

Substituting expansion (3.5) into Eq. (3.4) and equating powers of N yields the following hierarchy of equations:

$$\mathcal{O}(N^2) \ : \ -\partial_X^2 u_0 = 0, \tag{3.6}$$
$$\mathcal{O}(N) \ : \ -\partial_X^2 u_1 = 2\partial_x\partial_X u_0, \tag{3.7}$$
$$\mathcal{O}(N^0) \ : \ -\partial_X^2 u_2 = 2\partial_x\partial_X u_1 + \partial_x^2 u_0 + [1 + m(X)]u_0^p - \nu u_0, \tag{3.8}$$
$$\mathcal{O}(N^{-1}) : \ -\partial_X^2 u_3 = 2\partial_x\partial_X u_2 + \partial_x^2 u_1 + [1 + m(X)]pu_0^{p-1}u_1 - \nu u_1, \tag{3.9}$$
$$\mathcal{O}(N^{-2}) : \ -\partial_X^2 u_4 = 2\partial_x\partial_X u_3 + \partial_x^2 u_2 + [1 + m(X)]pu_0^{p-1}u_2$$
$$+ [1 + m(X)]\binom{p}{2}u_0^{p-2}u_1^2 - \nu u_2. \tag{3.10}$$

Similarly, substituting Eq. (3.5) into the boundary condition $\frac{d}{dx}u^{(N)}(0) = 0$, see Eq. (2.11), and equating powers of N gives the following hierarchy of boundary conditions:

$$\mathcal{O}(N) \quad : \quad \partial_X u_0(x = 0, X = 0) = 0, \tag{3.11}$$
$$\mathcal{O}(N^{-j}) \ : \ \partial_X u_{j+1}(0,0) + \partial_x u_j(0,0) = 0, \qquad j = 0, 1, ... \tag{3.12}$$

In addition, the condition $u^{(N)}(\infty) = 0$ translates into

$$u_j(\infty, X) = 0 \qquad j = 0, 1, ... \tag{3.13}$$

Each equation in the hierarchy (3.6)-(3.10) is of the form

$$-\partial_X^2 u_j(X; x) = F_j(x, X), \tag{3.14}$$

where $F_j(x, X)$ depends on $\{u_n\}_{n<j}$. Since $m(X)$ has period 1, we shall seek to construct an expansion where each u_j, and therefore each $F_j(x, X)$ has a period 1 in X. For this we use:

Lemma 4 *Equation (3.14), in which the forcing function $F_j(\cdot, X)$ is a periodic function of X with period 1, has a solution which is periodic in X with period 1 if and only if $\langle F_j \rangle = 0$. In this case, the solution of Eq. (3.14) can be explicitly constructed using the Fourier series of $F_j(\cdot, X)$.*

Proof: Since $F_j(\cdot, X)$ is periodic it can be expanded in a Fourier series:

$$F_j(\cdot, X) = \sum_{n\in\mathbb{Z}} f_n e^{i2\pi nX}.$$

If $\langle F_j \rangle = 0$, then we can define ∂_X^{-k}, a mapping from the space of mean zero

periodic functions to itself by:

$$\partial_X^{-k} F_j = \sum_{n\neq 0} (i2\pi n)^{-k} \ f_n e^{i2\pi nX}. \tag{3.15}$$

Note that $u_j(X) = -\partial_X^{-2} F_j(X)$ satisfies Eq. (3.14). Conversely, if $u_j(X)$ is a periodic solution of Eq. (3.14), then integration of Eq. (3.14) between 0 and 1 implies $\langle F_j \rangle = 0$. $\square$

Remark 5 *The general solution of Eq. (3.14) which satisfies the periodicity requirement $u_j(\cdot, X) = u_j(\cdot, X + 1)$ is*

$$u_j(X, x) = -\partial_X^{-2} F_j(X, x) + u_{j,h}(x),$$

where $u_{j,h}(x)$ is an arbitrary function of x and $\partial_X^{-2} F_j$ is defined by (3.15).

We now turn to solve Eqs. (3.6)-(3.10). By Remark 5, the solution of Eq. (3.6) is $u_0 = u_{0,h}(x)$ which indeed satisfies condition (3.11). Consequently, the solution of Eq. (3.7) is

$$u_1 = u_{1,h}(x). \tag{3.16}$$

By Lemma 4, solvability of Eq. (3.8) requires that the average of its right-hand-side would be equal to zero. Since, $u_0 = u_{0,h}$, this yields

$$\partial_x^2 u_{0,h} + u_{0,h}^p - \nu u_{0,h} = 0. \tag{3.17}$$

Hence, by conditions (3.12) and (3.13), $u_0 = u_{0,h} = \mathcal{U}(x, \nu)$, see Eq. (2.10). Since, in addition, $u_1 = u_{1,h}(x)$, from Eq. (3.8) it follows that $u_2(x, X)$ satisfies the simplified equation

$$-\partial_X^2 u_2 = m(X)\mathcal{U}^p(x, \nu).$$

By Remark 5,

$$u_2 = -\mathcal{U}^p(x, \nu)\,[\partial_X^{-2} m(X)] + u_{2,h}(x), \qquad (3.18)$$

where the homogeneous solution, $u_{2,h}(x)$, is to be determined at a later stage and $\partial_X^{-2} m(X)$ is defined by (3.15). Consequently, condition (3.12) for $j = 1$ becomes

$$\partial_X u_2(0,0) + \partial_x u_1(0,0) = -\mathcal{U}^p(0, \nu)\,[\partial_X^{-1} m(X)]\big|_{x=0} + \partial_x u_{1,h}(0)$$
$$= \partial_x u_{1,h}(0) = 0. \qquad (3.19)$$

Solvability of Eq. (3.9) requires that the $X-$ average of its right-hand-side would be equal to zero. Using Eq. (3.16) gives

$$L_+ u_{1,h} = 0, \qquad (3.20)$$

where L_+ is given by Eq. (3.3). Since L_+ has the null space

$$Ker(L_+) = \mathrm{span}\{\partial_x \mathcal{U}(x, \nu)\}, \qquad (3.21)$$

and since $\partial_x \mathcal{U}(x, \nu)$ is an odd function of x, the solution of Eq. (3.20) subject to the boundary conditions (3.19) and (3.13) is $u_{1,h} \equiv 0$. Therefore, by Eq. (3.16), $u_1 \equiv 0$. Therefore, by Remark 5 and Eq. (3.18), the solution of Eq. (3.9) is given by

$$u_3(x, X) = 2\,(\partial_X^{-3} m(X))\,\partial_x(\mathcal{U}^p) + u_{3,h}(x), \qquad (3.22)$$

and condition (3.12) for $j = 2$ becomes

$$\partial_x u_2(0,0) = 0. \qquad (3.23)$$

Solvability of Eq. (3.10) requires that the $X-$ average of the terms on its right-hand-side would be equal to zero. Calculating the averages term by term gives

$$\langle 2\partial_x \partial_X u_3 \rangle = 0, \qquad (3.24)$$

for the first term. Using Eq. (3.18), gives

$$\partial_x^2 u_2 - \nu u_2 = -[\partial_X^{-2} m(X)]\left(\partial_x^2 - \nu\right)\mathcal{U}^p(x, \nu) + \left(\partial_x^2 - \nu\right)u_{2,h}(x),$$

whose average is given by

16

$$\langle \partial_x^2 u_2 - \nu u_2 \rangle = \left(\partial_x^2 - \nu \right) u_{2,h}(x). \tag{3.25}$$

In the same manner, by Eq. (3.18)

$$\left\langle (1 + m(X))\, p\mathcal{U}^{p-1} u_2 \right\rangle = \left\langle (1 + m(X)) p\mathcal{U}^{p-1}\left(-[\partial_X^{-2} m(X)]\mathcal{U}^p + u_{2,h}(x) \right) \right\rangle$$
$$= p\mathcal{U}^{p-1} u_{2,h}(x) + p\tau_m \mathcal{U}^{2p-1}, \tag{3.26}$$

where τ_m is given by Eq. (3.2). Substituting the averages (3.24), (3.25) and (3.26) in the X-average of the right-hand-side of Eq. (3.10) gives the following equation for $u_{2,h}(x)$

$$\partial_x^2 u_{2,h} - \nu u_{2,h} + p\mathcal{U}^{p-1}(x, \nu) u_{2,h} + p\tau_m \mathcal{U}^{2p-1} = 0.$$

Therefore, by condition (3.23),

$$u_{2,h}(x) = p\,\tau_m L_+^{-1}[\mathcal{U}^{2p-1}]\,,$$

where L_+ is defined by Eq. (3.3). Finally, by Eq. (3.18),

$$u_2(x, X) = -[\partial_X^{-2} m(X)]\,\mathcal{U}^p(x, \nu) + p\tau_m\, L_+^{-1}[\mathcal{U}^{2p-1}]. \tag{3.27}$$

This concludes the proof of Theorem 3. □.

We can use the results of Theorem 3 to calculate the effect of a periodic nonlinear microstructure on the power (L^2 norm) of the bound states $\|u^{(N)}(\nu)\|_2^2 = \int |u^{(N)}(x, \nu)|^2 dx$:

Corollary 6 *Let $u^{(N)}$ be the solution of Eq. (2.11), let $m(X)$ satisfy Eq. (2.7) and let $N \gg 1$. Then,*

$$\|u^{(N)}(\nu)\|_2^2 = \|\mathcal{U}(\nu)\|_2^2 - \frac{C_{wide}}{N^2} + \mathcal{O}(N^{-4}), \tag{3.28}$$

where the constant C_{wide} is given by $C_{wide} = \tau_m \partial_\nu \int \mathcal{U}^{2p}(x, \nu)\, dx$ and τ_m is given by Eq. (3.2).

Proof: See Appendix A.

Corollary 6 implies the following

Theorem 7 *Let $N \gg 1$. Then, a mean-zero nonlinear microstructure always decreases the L^2 norm (power) of the bound states of Eq. (2.4), i.e., $\|u^{(N)}(\nu)\|_2^2 < \|\mathcal{U}(\nu)\|_2^2$.*

Proof: Recall that $\mathcal{U}(x, \nu)$ satisfies, see Eq.(2.10),

$$\mathcal{U}(x, \nu) \;=\; \nu^{\frac{1}{p-1}} \mathcal{U}(\nu^{\frac{1}{2}} x, 1). \tag{3.29}$$

Hence,

$$\int \mathcal{U}(x, \nu)^{2k} \, dx = \nu^{\frac{2k}{p-1} - \frac{1}{2}} \rho_*(k), \qquad \rho_*(k) = \int \mathcal{U}^{2k}(x, 1) \, dx > 0, \tag{3.30}$$

which for $k = p$ reduces to $\nu^{\frac{2p}{p-1} - \frac{1}{2}} \rho_*(p)$. Therefore, for all $p > 1$ and $\nu > 0$,

$$\begin{aligned}
\partial_\nu \int \mathcal{U}(x, \nu)^{2p} \, dx &= \left(\frac{2p}{p-1} - \frac{1}{2} \right) \nu^{\frac{2p}{p-1} - \frac{3}{2}} \, \rho_*(p) \\
&= \left(\frac{3p+1}{2(p-1)} \right) \nu^{\frac{2p}{p-1} - \frac{3}{2}} \, \rho_*(p) > 0.
\end{aligned} \tag{3.31}$$

Hence, the $\mathcal{O}(N^{-2})$ term in Eq. (3.28) is strictly negative. $\square$.

3.1.1 Simulations

In this section, we solve the boundary value problem (2.11) numerically using the Fourier transform iterative method (see Appendix B). These simulations confirm the results of the multiple scale analysis for $N \gg 1$. In fact, we observe that even for $N \approx 2$ there is a good agreement between the results of the multiple scale expansion and the computed bound states.

In the simulations we use the nonlinear microstructure

$$m = \alpha \cos(2\pi N x) = \alpha \cos(2\pi X), \tag{3.32}$$

which satisfies conditions (2.7). In this case, $\alpha > 0$ ($\alpha < 0$) describes a situation where the beam is centered at a local maximum (minimum) of the nonlinear microstructure and $|\alpha|$ expresses the relative magnitude of microstructure variations.

The solutions of Eq. (2.11) for $\nu = 1$ and $\alpha = \pm 0.5$ are shown in Fig. 2 for various values of N in the subcritical case $p = 3$. Note that even for $N = 2$ and $\mathcal{O}(1)$ changes in the nonlinear microstructure, $u^{(N)}$ is nearly indistinguishable from the homogeneous medium soliton $\mathcal{U}$. Indeed, plotting the difference $u^{(N)} - \mathcal{U}$ shows that the microstructure adds a small modulation whose magnitude scales as N^{-2}, and whose local period is N, as predicted by Theorem 3. **Moreover, u_2/N^2, the leading order correction to $\mathcal{U}$ is in excellent agreement with the numerical values of the difference of $u^{(N)} - \mathcal{U}$.**
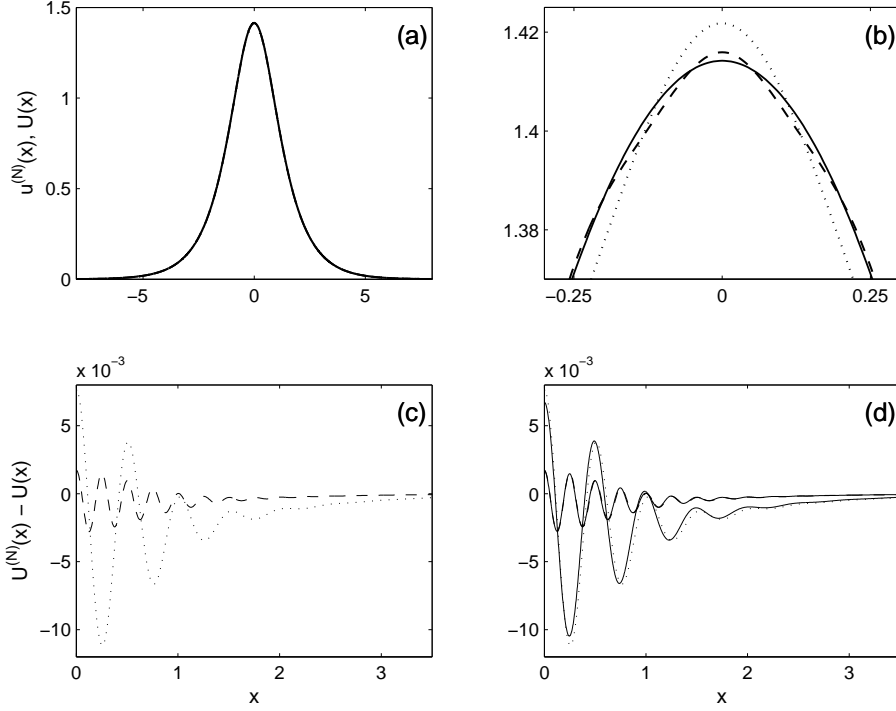
18

Fig. 2. Solutions of Eq. (2.11) with $p = 3$, $\nu = 1$ and $m = 0.5\cos(2\pi Nx)$ for $N = 2$ (dotted line) and $N = 4$ (dashed line). Also shown is $\mathcal{U} = \sqrt{2}\mathrm{sech}(x)$ (solid line). (a) $u^{(N)}$ and $\mathcal{U}$ as a function of x: all three lines are indistinguishable. (b) Magnification of region near $x = 0$. (c) $u^{(N)} - \mathcal{U}$ as a function of x. (d) Same as (c). Also shown is u_2/N^2 as given by Eq. (3.27) (solid line).

Fig. 3 shows the difference between $\|\mathcal{U}\|_2^2 = 4$ and $\|u^{(N)}\|_2^2$ for $\nu = 1$ and $2 \leq N \leq 15$. The microstructure causes the L^2 norm of $u^{(N)}$ to decrease, as predicted by Theorem 7. In order to quantitatively assess the accuracy of the multiple-scales/homogenization expansion, we recall that according to Corollary 6,

$$\|\mathcal{U}\|_2^2 - \|u^{(N)}\|_2^2 \approx C_{wide}N^{-2}, \tag{3.33}$$

where for $p = 3$,

$$C_{wide} \equiv \underbrace{\frac{\alpha^2}{(2\pi)^2}\int_0^1 (\sin 2\pi X)^2 dX}_{\tau_m}\ \partial_\nu \int_{-\infty}^{\infty} \mathcal{U}^6(x, \nu = 1)dx = \frac{2}{3\pi^2}.$$

Therefore, $\log(\|\mathcal{U}\|_2^2 - \|u^{(N)}\|_2^2) \approx \log(C_{wide}) - \beta\ \log(N)$ with $\beta = 2$ and $\log(C_{wide}) \approx -2.695$. A least square fit of the numerical data gives $\beta = 2.0035$ and $\log(C_{wide}) = -2.684$, i.e., less than 1% difference. Since there is excellent agreement between Corollary 6 and the numerical data up to $N = 2$, we conclude that the results of the multiple scale expansion remain valid for

values of N that are only moderately above one.

Remark 8 *We recall that N was defined as the ratio of the beam radius r_{beam} to the microstructure period r_{ms}. Hence, $N = 2$ corresponds to a beam that extends over $2N = 4$ microstructure periods. Therefore, the agreement of the multiple scales expansion with the numerics for values of N as small as 2 is to be expected.*
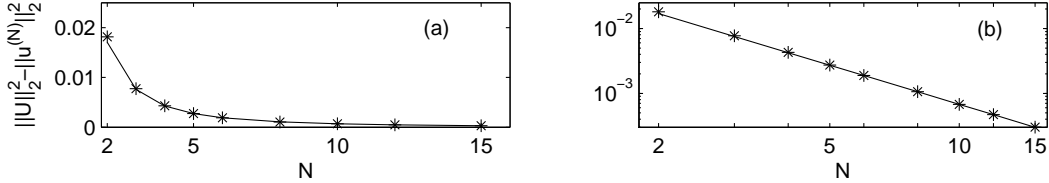

Fig. 3. A: Difference between the power of $\mathcal{U}$ and $u^{(N)}$ for $p = 3$ and $\alpha = \pm 0.5$ (stars) and least square fit of $\log(||\mathcal{U}||_2^2 - ||u^{(N)}||_2^2) \approx -2.0035 \ \log N - 2.68$ (solid line). B: same data on a log-log scale.

In Fig. 4 we show solution of Eq. (2.11) for $\alpha < 0$, i.e., bound states centered at a local minimum of the microstructure. For $\alpha = -0.3$ the bound state has a global maximum at $x = 0$. However, for smaller values of α (e.g. $\alpha = -0.8$), bound states have a local minimum at $x = 0$ and two adjacent global maxima. We note that Eq. (2.11) has solutions also for $\alpha < -1$, i.e., for the case of a medium which consists of both focusing and defocusing regions. Indeed, the multiple scales expansion shows that the effective nonlinearity is only determined only by the *average* nonlinear coefficient (which is independent of α). Hence, the microstructure can support bound states also for $\alpha < -1$.
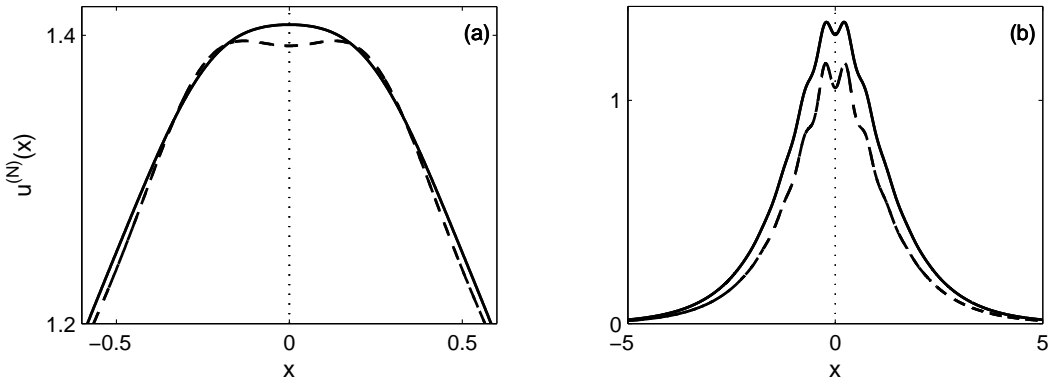

Fig. 4. Solutions of Eq. (2.11) with $p = 3$, $\nu = 1$ and $m = 0.5 \cos(2\pi N x)$ for $N = 2$. (a) $\alpha = -0.3$ (solid line) and $\alpha = -0.8$ (dashed line). (b) $\alpha = -3$ (solid line) and $\alpha = -8$ (dashed line).

20

We now consider the case of narrow beams, i.e., $N \ll 1$ or $r_{beam} \ll r_{ms}$. In this case, the beam is influenced mainly by the local changes of the microstructure near the beam center, and not by the global periodic structure.

As before, we assume that $m(X)$ satisfies conditions (2.7). Using a perturbation analysis similar to the one in [21], we show in Appendix C that the solution of Eq. (2.11) is given by

$$u^{(N)}(x; \nu) = [1 + m(0)]^{-\frac{1}{p-1}} \left[\mathcal{U}(x, \nu) + N^2 \frac{m''(0)}{2} L_+^{-1}(x^2 \mathcal{U}^p) \right] + \mathcal{O}(N^4), \quad (3.34)$$

where $\mathcal{U}$ is given by Eq. (2.10) and L_+ is by Eq. (3.3). By Eq. (C.17), the power of $u^{(N)}$ is given by

$$\|u^{(N)}(\nu)\|_2^2 = [1 + m(0)]^{-\frac{2}{p-1}} \left(\|\mathcal{U}(\nu)\|_2^2 + \frac{N^2}{\nu} \frac{(p-5)m''(0) \int x^2 \mathcal{U}^{p+1}}{2[1 + m(0)](p^2 - 1)} \right)$$
$$+ \mathcal{O}(N^4). \quad (3.35)$$

Thus, for $p \neq 5$, the microstructure induces an $\mathcal{O}(N^2)$ change in the bound state power, whose sign is given by $sgn[(p-5)m''(0)]$. In the critical case $p = 5$, the contribution of the $\mathcal{O}(N^2)$ term vanishes and by Eq. (C.18),

$$\|u^{(N)}(\nu)\|_2^2 = \frac{\|\mathcal{U}(\nu)\|_2^2}{[1 + m(0)]^{\frac{1}{2}}} \quad (3.36)$$
$$- \frac{N^4}{\nu} \frac{\int x^4 \mathcal{U}^6(x, \nu)}{72[1 + m(0)]^{\frac{5}{2}}} \left[[m''(0)]^2 G_5 - m^{(4)}(0)[1 + m(0)] \right] + \mathcal{O}(N^6),$$

where

$$G_5 = -18 \frac{\int x^2 \mathcal{U}^5 L_+^{-1}[x^2 \mathcal{U}^5]}{\int x^4 \mathcal{U}^6} \cong -0.3531, \quad (3.37)$$

is a ν-independent constant. Thus, in the critical case, the leading order effect of the nonlinear microstructure on the bound state profile is $\mathcal{O}(N^2)$ but its effect on the power is only $\mathcal{O}(N^4)$, as was first pointed out in [21]. In addition, unlike the subcritical ($p < 5$) and supercritical ($p > 5$) cases, the sign of the $\mathcal{O}(N^4)$ correction does not depend only on the sign of $m''(0)$, i.e., on whether m has a local maximum or minimum at $x = 0$, but also on the magnitude of $m''(0)$ and on the values of $m(0)$ and $m^{(4)}(0)$.

3.2.1 Simulations

As in the wide beam case, we solve the boundary value problem (2.11) numerically using the Fourier transform iterative method (see Appendix B) and confirm the validity of the perturbation analysis for $N \ll 1$. The solutions of Eq. (2.11) with $m(X) = \alpha \cos(2\pi X)$ and $p = 5$ are shown in Fig. 5 for $N = 0.1, 0.2$, and 0.4. As predicted by Eq. (3.34), the difference between $u^{(N)}$ and $\mathcal{U}$ scales as N^2. From Eq. (3.30) and Eq. (3.36) it follows that the power dependence on N is given by
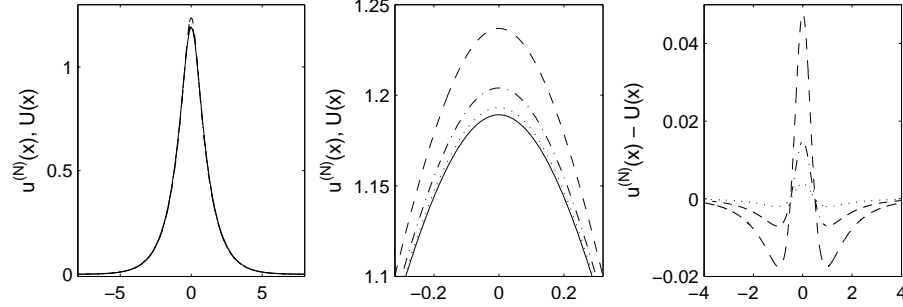

Fig. 5. Solutions of Eq. (2.11) with $p = 5$, $\nu = 1$ and $m = 0.5 \cos(2\pi N x)$ for $N = 0.1$ (dotted line), $N = 0.2$, (dash-dotted line) and $N = 0.4$ (dashed line). Also shown is $\mathcal{U} = 3^{\frac{1}{4}} \operatorname{sech}^{\frac{1}{2}}(2x)$ (solid line). (a) $u^{(N)}$ and $\mathcal{U}$ as a function of x: all three lines are indistinguishable. (b) Magnification of region near $x = 0$. (c) $u^{(N)} - \mathcal{U}$ as a function of x.

$$||u^{(N)}||_2^2 - \frac{||\mathcal{U}||_2^2}{[1 + m(0)]^{\frac{1}{2}}} \approx C_{narrow} \frac{N^4}{\nu^2}, \tag{3.38}$$

where

$$C_{narrow} \equiv \frac{\int_{-\infty}^{\infty} x^4 \, \mathcal{U}^6(x, 1)}{72 \, [1 + m(0)]^{\frac{5}{2}}} \left(\left[1 + m(0)\right] m^{(4)}(0) - G_5[m''(0)]^2 \right), \tag{3.39}$$

and where $\mathcal{U}(x, 1)$ is given by Eq. (2.10). Since $m(X) = \alpha \cos(2\pi X)$, we can rewrite C_{narrow} as

$$C_{narrow} = \tilde{C}_{narrow} \frac{\alpha}{[1 + \alpha]^{\frac{5}{2}}} (\alpha + \alpha_c), \tag{3.40}$$

where $\tilde{C}_{narrow} = (2\pi)^4 \, (1 - G_5) \int_{-\infty}^{\infty} x^4 \, \mathcal{U}^6(x, 1)/72 \cong 3.39$ and $\alpha_c = \frac{1}{1 - G_5} \cong 0.7390$. Therefore, C_{narrow} is positive if and only if $0 > \alpha > -\alpha_c$. Fig. 6 demonstrates the change in the power of the bound states for $\alpha = 0.5 > 0$, $0 > \alpha = -0.5 > -\alpha_c$ and $\alpha = -0.9 < -\alpha_c$. As predicted by Eqs. (3.38)-(3.40), the power of the bound state decreases with N in the second case and increases in the first and third cases. Additionally, from Eq. (3.38) it follows that $\log \left(||u^{(N)}||_2^2 - ||\mathcal{U}(x, 1)||_2^2/(1 + \alpha) \right) \approx \log(C_{narrow}) - \beta \, \log(N)$ with $\beta = 4$

and C_{narrow} is given by Eq. (3.40). A least square fit of the data of Fig. 6 yielded these values of β and C_{narrow} with $2\% - 4\%$ accuracy.
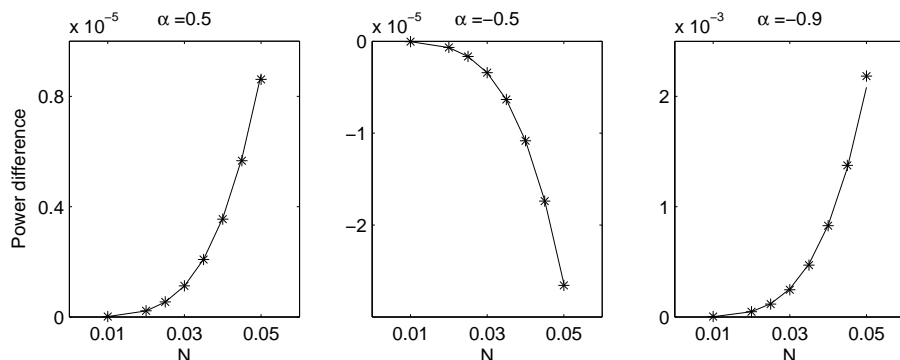

Fig. 6. Power difference $\|u^{(N)}\|_2^2 - \|\mathcal{U}(x, nu)\|_2^2/(1 + \alpha)^{1/2}$ for $p = 5$, $\nu = 1$ and $\alpha = 0.5$, $\alpha = -0.5$ and $\alpha = -0.9$. Solid line is the least square fit of $C_{narrow}N^\beta$.

4 Stability of bound states - analysis

4.1 Conditions for stability

We now analyze the stability of the waveguide solutions $\phi_{wg} = e^{i\nu z}u^{(N)}(x; \nu)$, where $u^{(N)}$ is the solution of Eq. (2.11).

In the case of the NLS with a nonlinear microstructure (2.4), the appropriate notion of stability, *orbital stability*, is as follows: [2]

Definition 9 *Let $u^{(N)}(x; \nu)$ be a solution of Eq. (2.11). Then, $\phi_{wg}(x, z) = u^{(N)}(x; \nu)e^{i\nu z}$ is an orbitally stable solution of Eq. (2.4) if $\forall \epsilon$, $\exists \delta > 0$ such that for any $\phi(x, 0) \in H^1(\mathbb{R}^1)$ which satisfies $\inf_\theta \|\phi(\cdot, 0) - u^{(N)}e^{i\theta}\|_{H^1} < \delta$, the corresponding solution $\phi(x, z)$ of Eq. (2.4) satisfies*

$$\sup_{z \geq 0} \inf_\theta \|\phi(\cdot, z) - \phi_{wg}e^{i\theta}\|_{H^1} < \epsilon.$$

The following result on nonlinear stability and instability was proved in [29,56,57]:

---

[2] Under the definition of orbital stability, the solution remains close to the family of all the transformations of the solitary wave which leaves the equation invariant. In the presence of nonlinear microstructure, the only such transformation is a phase shift.

Theorem 10 *Let $u^{(N)}$ be **a positive** solution of Eq. (2.11) and let $n_-(L_+^{(N)})$ be the number of negative eigenvalues of the operator*

$$L_+^{(N)} = -\partial_x^2 + \nu - p(1 + m(Nx))\left(u^{(N)}(x)\right)^{p-1}. \tag{4.1}$$

Then, $\phi_{wg} = u^{(N)}(x; \nu)e^{i\nu z}$ is a nonlinearly orbitally stable solution of Eq. (2.4) if and only if

(S1) $n_-(L_+^{(N)}) \leq 1$ (spectral condition).
(S2) $\partial_\nu \|u^{(N)}(x; \nu)\|_2^2 > 0$ (slope condition).

Furthermore, the failure of either (S1) or (S2) implies the existence of an exponentially growing solution of the linearized NLS dynamics [28,33].

Remark 11 ***The* spectral condition *in [29,56,57] is***

$$n_-(L_+^{(N)}) - n_-(L_-^{(N)}) \leq 1, \tag{4.2}$$

where $n_-(L_-^{(N)})$ is the number of negative eigenvalues of the operator

$$L_-^{(N)} = -\partial_x^2 + \nu - (1 + m(Nx))\left(u^{(N)}(x)\right)^{p-1}. \tag{4.3}$$

Since $L_-^{(N)}u^{(N)} = 0$, and since the smallest eigenvalue of $L_-^{(N)}$ is attained by a positive function, we conclude that $n_-(L_-^{(N)}) = 0$ if and only if $u^{(N)} > 0$. In that case, the spectral condition reduces to (S1).

Remark 12 ***In Section 2, we showed that $u^{(N)} = \mathcal{U} + o(1)$ for $N \gg 1$ and $N \ll 1$. Since $\mathcal{U} > 0$, we conclude that $u^{(N)} > 0$ for $N \gg 1$ and $N \ll 1$. In addition, in all our numerical simulations for $N = \mathcal{O}(1)$ beams, we also observe that $u^{(N)} > 0$. Therefore, it is reasonable to assume in Theorem 10 that $u^{(N)}$ is positive. Clearly, if Eq. (2.11) admits solutions which are not positive (i.e., solutions for which $\mathcal{U}$ is not the leading order term in the solution) the correct spectral condition is (4.2) rather than (S1).***

We now remark on the idea behind the proof. Conditions (S1) and (S2) stem from a *variational* characterization of bound states. The variational approach is based on the observation that bound states of microstructure NLS are critical points of the energy functional

$$\mathcal{E}_\nu[f] \equiv \mathcal{H}[f] + \nu\mathcal{P}[f]. \tag{4.4}$$

Here,

$$\mathcal{H} = \int \left(|\partial_x f(x)|^2 - \frac{2}{p+1}(1 + m(Nx))|f(x)|^{p+1} \right) \, dx$$

and

$$\mathcal{P} = \int |f(x)|^2 \, dx \tag{4.5}$$

are conserved integrals of NLS [3]. Note that if U is a stationary point of $\mathcal{H}$ subject to fixed $\mathcal{P}$, then U is a critical point of $\mathcal{E}_\nu$ for some Lagrange multiplier ν, and moreover U satisfies equation (2.11). In [29,56,57] it is shown that for a bound state to be nonlinearly orbitally stable it is essentially necessary and sufficient for it to be a local minimizer of $\mathcal{H}$ subject to fixed $\mathcal{P}$.

At the heart of Theorem 10 is a study of whether $\mathcal{Q}(U)$, the second variation (Hessian) of the functional $\mathcal{E}_\nu$ about U, constrained to the subspace $\mathcal{C}$, which is defined in terms of orthogonality conditions related to the conserved integrals of NLS, is positive. $\mathcal{Q}$ is defined as

$$\mathcal{Q}(U) = \langle L_+^{(N)} f, f \rangle + \langle L_-^{(N)} g, g \rangle, \quad U = f + ig, \tag{4.6}$$

where $L_+^{(N)}$ and $L_-^{(N)}$ are second order Schrödinger operators associated with the real and imaginary parts of the operators.

In [56,57] it was shown that positivity of $\mathcal{Q}$ on $\mathcal{C}$ (and therefore orbital stability) holds if and only if (S1) and (S2) hold. In [28,33] general results were derived for the number of exponentially growing (in z) modes of the linearized dynamics for NLS in terms of the number of negative eigenvalues of $L_+^{(N)}$ and $L_-^{(N)}$. In particular, the failure of either (S1) or (S2) implies the existence of an exponentially growing solution of the linearized dynamics.

4.2   Stability in a homogeneous medium

In the case of a homogeneous medium (i.e., $m(x) \equiv 0$), $u^{(N)}$ reduces to $\mathcal{U}$, see Eq. (2.10), and the operator $L_+^{(N)}$ reduces to L_+ as given in Eq. (3.3). The associated eigenvalue problem of the linearized operators L_+ is

$$L_+ f = \lambda f, \quad -\infty < x < \infty, \qquad f(x = \pm\infty) = 0. \tag{4.7}$$

The spectrum of L_+ is composed of (see e.g., [56]),

---

[3] The idea is motivated by the seminal article of T.B. Benjamin on the stability of the KdV soliton [10].

(1) A simple negative eigenvalue, denoted by λ_{min}, with an even eigenfunction $f_{min}(x)$.
(2) A simple eigenvalue $\lambda_0 = 0$, with the corresponding odd eigenfunction $f_0(x) = \partial_x \mathcal{U}$.
(3) A strictly positive continuous spectrum $[\nu, \infty)$.

Thus, $n_-(L_+) = 1$, and stability is determined by the slope condition. By Eq. (3.30),

$$\begin{cases} \partial_\nu \|\mathcal{U}(\nu)\|_2^2 > 0, & p < 5, \\ \partial_\nu \|\mathcal{U}(\nu)\|_2^2 = 0, & p = 5, \\ \partial_\nu \|\mathcal{U}(\nu)\|_2^2 < 0, & p > 5. \end{cases} \tag{4.8}$$

Thus, by Theorem 10, $\phi_{wg} = e^{i\nu z}\mathcal{U}$ is stable for $p < 5$ and unstable for $p \geq 5$.

4.3   Spectral condition (S1)

We now use Theorem 10 to determine the stability of waveguide solutions of Eq. (2.4). We first state two Propositions which are consequences of basic ODE theory; see, for example, [16].

Proposition 13 *The eigenvalues of the self-adjoint operator $L_+^{(N)}$ are real and simple.*

Proposition 14 *The eigenvalues and eigenfunctions of $L_+^{(N)}$ vary analytically with N.*

We now prove the following result:

Proposition 15 *The eigenfunctions of $L_+^{(N)}$ are either even or odd.*

Proof: Let $f^{(N)}$ be the eigenfunction of the operator $L_+^{(N)}$, i.e.,

$$L_+^{(N)} f^{(N)}(x) = \lambda^{(N)} f^{(N)}(x).$$

Then, since $L_+^{(N)}$ is even,

$$L_+^{(N)} f(-x) = \lambda^{(N)} f^{(N)}(-x).$$

Hence,
$$L_+^{(N)}[f^{(N)}(x) \pm f^{(N)}(-x)] = \lambda^{(N)}[f^{(N)}(x) \pm f^{(N)}(-x)].$$

Thus, by Proposition 13 it follows that either $[f^{(N)}(x) + f^{(N)}(-x)] \equiv 0$ or $[f^{(N)}(x) - f^{(N)}(-x)] \equiv 0$. Hence, f must be either odd or even. $\square$

26

Using these properties, we now study the spectrum of $L_+^{(N)}$. We note that the coefficients of $L_+^{(N)}$ converge to those of $L_+^{(0)}$ as $N \to 0$, where $L_+^{(0)}$ is the linearized operator that corresponds to

$$i\partial_z \phi = -\partial_x^2 \phi - (1 + m(0))|\phi|^{p-1}\phi.$$

Since this equation reduces to Eq. (2.5) through a simple scaling, the properties of the eigenfunctions and eigenvalues of $L_+^{(0)}$ aresimilar to those of L_+. In addition, by Propositions 13 and 14, it follows that the structure of the spectrum of $L_+^{(N)}$ is similar to the spectrum of $L_+^{(0)}$, i.e., two simple discrete eigenvalues (denoted by $\lambda_{min}^{(N)}$ and $\lambda_0^{(N)}$, respectively) and a continuous spectrum $[\nu^{(N)}, \infty)$. In the following Theorem we determine the signs of $\lambda_{min}^{(N)}$ and the continuous spectrum:

Proposition 16 *Let $L_+^{(N)}$ be given by Eq. (4.1) and let $m(Nx)$ satisfy Eq. (2.7). Then, $\lambda_{min}^{(N)} < 0$ and $\nu^{(N)} > 0$.*

Proof: Let $f_* = u^{(N)} / \|u^{(N)}\|_2$. Since $u^{(N)}$ is the solution of Eq. (2.11), the Rayleigh quotient of f_* is

$$\langle L_+^{(N)} f_*, f_* \rangle = \frac{1}{\|u^{(N)}\|_2^2} \langle \left(-\partial_x^2 - p(1 + m(Nx))u^{(N)p-1} + \nu \right) u^{(N)}, u^{(N)} \rangle$$

$$= -\frac{p-1}{\|u^{(N)}\|_2^2} \langle (1 + m(Nx))u^{(N)p}, u^{(N)} \rangle < 0.$$

Hence, from the variational characterization of the principal eigenvalue of $L_+^{(N)}$ [16,45],

$$\lambda_{min}^{(N)} \equiv \inf_{f \in H^1} \frac{\langle L_+^{(N)} f, f \rangle}{\langle f, f \rangle} < 0.$$

Concerning the continuous spectrum, note that $L_+^{(N)}$ is a Schrödinger operator of the form

$$-\partial_x^2 + \nu + V(x), \quad V(x) = -p(1 + m(Nx)) \left(u^{(N)p-1}(x) \right).$$

Since $V(x)$ decays to zero rapidly at infinity, it follows by Weyl's theorem on the stability of the essential spectrum, which here equals the continuous spectrum, that the continuous spectrum of $L_+^{(N)}$ is equal to that of the "operator at infinity" $-\partial_x^2 + \nu$ [45]. The latter is given by the semi-infinite interval $[\nu, \infty)$. $\square$

We thus see that the discrete eigenvalue $\lambda_0^{(N)}$ to which the simple eigenvalue $\lambda_0 = 0$ perturbs, determines whether $n_- = 1$ or $n_- = 2$. We recall

that λ_0 is related to the translation invariance of solutions of Eq. (2.10). Indeed, since $\mathcal{U}(x + \delta)$ is a solution of Eq. (2.10) for all δ, differentiation of Eq. (2.10) with respect to δ implies $L_+\mathcal{U}_x = 0$, $i.e.$ $\partial_x\mathcal{U}$ is an eigenfunction of L_+ with eigenvalue $\lambda_0 = 0$. However, in the presence of microstructure ($m(x) \not\equiv 0$), the bound state equation (2.11) is no longer translation invariant. Thus, we expect $L_+^{(N)}$ not to have a zero eigenvalue.

Since f_0 is odd, it follows from Proposition 14 and Proposition 15 that $f_0^{(N)}$ is odd for all N. Similarly, since $f_{min}^{(N)}$ is even, the eigenfunction that corresponds to the negative eigenvalue, $\lambda_{min}^{(N)}$ is even. Hence, it is useful to distinguish between the

(1) *Symmetric problem*, i.e., when the solution of Eq. (2.4) satisfies $\phi(z, x) = \phi(z, -x)$.
(2) *General, asymmetric problem.*

The eigenvalue problem of the linear stability operator $L_+^{(N)}$ of the NLS with nonlinear microstructure (2.4) in the symmetric problem is

$$L_+^{(N)} f^{(N)}(x) = \lambda f^{(N)}, \quad 0 < x < \infty, \qquad f_x^{(N)}(0) = 0, \quad f^{(N)}(\infty) = 0,$$
$$(4.9)$$

and in the asymmetric problem is

$$L_+^{(N)} f^{(N)}(x) = \lambda f^{(N)}, \quad -\infty < x < \infty, \qquad f^{(N)}(\pm\infty) = 0. \qquad (4.10)$$

In both cases, $L_+^{(N)}$ is given by Eq. (4.1). It follows from Proposition 15 that the eigenvalues of $L_+^{(N)}$ in the symmetric problem (4.9) consist only of the eigenvalues of $L_+^{(N)}$ in the general (asymmetric) problem (4.10), for which the corresponding eigenfunctions are even. Specifically, the eigenvalue $\lambda_0^{(N)}$ of the general problem (4.10) is not an eigenvalue of the symmetric problem (4.9). Therefore, we have the following result:

Corollary 17 *Let $L_+^{(N)}$ be given by Eq. (4.1), let $m(Nx)$ satisfy Eq. (2.7). Then, in the symmetric problem (4.9), $n_-(L_+^{(N)}) = 1$.*

In the general (asymmetric) problem, we have to determine the sign of $\lambda_0^{(N)}$. For $N \ll 1$, we show in Appendix D that

$$\lambda_0^{(N)} = -C_p m''(0) N^2 + \mathcal{O}(N^4), \qquad (4.11)$$

where C_p is a positive constant for $p > 1$. Hence, $sgn(\lambda_0^{(N)}) = -sgn(m''(0))$ and we have the following result:

m(X)	$\alpha = 0.5$ (local maximum)		$\alpha = -0.5$ (local minimum)	
	$p = 3$	$p = 5$	$p = 3$	$p = 5$
$\alpha\cos(2\pi X)$	0.22	0.91	-0.23	-1.93
$\alpha(e^{-(X/0.1)^2} - 0.1772)$	0.07	0.47	-0.06	-0.57
$\alpha(e^{-(X/0.2)^4} - 0.3626)$	0.12	0.68	-0.12	-1.01
step function	0.13	0.72	-0.13	-1.16

Table 3
Eigenvalue $\lambda_0^{(N)}$ for $N = 1$, $p = 3$ and 5 and $\alpha = \pm 0.5$ for four different nonlinear microstructures.

Corollary 18 *Let $L_+^{(N)}$ be given by Eq. (4.1), let $N \ll 1$, let $m''(0) \neq 0$. Then, in the asymmetric problem (4.10),*

(1) $n_-(L_+^{(N)}) = 1$ for a beam centered at a local maximum of the microstructure ($m''(0) < 0$).
(2) $n_-(L_+^{(N)}) = 2$ for a beam centered at a local minimum of the microstructure ($m''(0) > 0$).

The parameter region which is not covered by theory is $N = \mathcal{O}(1)$, i.e., beams whose width is of the order of the microstructure period. In the absence of theory, we calculate $n_-(L_+^{(N)})$ numerically through direct discretization of $L_+^{(N)}$. We repeat the calculation for four different nonlinear microstructures that range from a very smooth microstructure to the discontinuous step function, see Fig. 7. In Table 3 we show $\lambda_0^{(N)}$ for $N = 1$, $p = 3$ and 5, and $\alpha = \pm 0.5$. As in the case of narrow beams, $\lambda_0^{(N)}$ is positive (negative) for a bound state centered at a local maximum (minimum) of the microstructure. Therefore, we conjecture that Corollary 18 holds also for $\mathcal{O}(1)$ beams (but see Section 4.5).
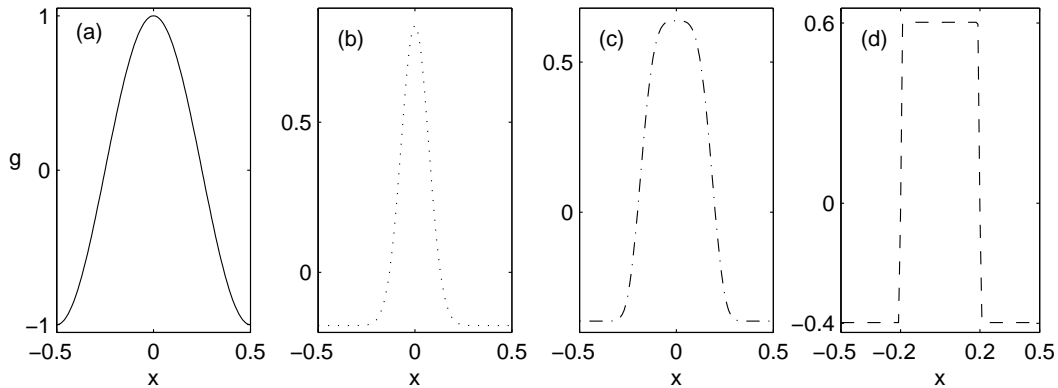

Fig. 7. One period of the mean-zero microstructures used in the simulations when $N = \mathcal{O}(1)$. (a) $m = \alpha\cos(2\pi X)$; (b) $m = \alpha(e^{-(X/0.1)^2} - 0.1772)$; (c) $m = \alpha(e^{-(X/0.2)^4} - 0.3626)$; (d) step function. In all plots $\alpha = 1$.

For $N \gg 1$ and $p > 1$, a multiple scales expansion shows that if we expand

$$\lambda_0^{(N)} = \frac{\lambda_1}{N} + \frac{\lambda_2}{N^2} + \cdots,$$

then $\lambda_1 = \lambda_2 = 0$ (see Appendix E). Therefore we conclude that $\lambda_0^{(N)} = o(N^{-2})$ but at present the sign of $\lambda_0^{(N)}$ remains undetermined analytically.

In order to demonstrate the dependence of $\lambda_0^{(N)}$ on N, we set $m = \alpha \cos(2\pi Nx)$ and calculate $\lambda_0^{(N)}$ numerically for the general eigenvalue problem (4.10), with no assumptions on symmetry, for values of N as large as our numerical solver permits. The results are shown in Fig. 8 for the critical case ($p = 5$). Results for the subcritical case are similar (data not shown). For $N \ll 1$, $\lambda_0^{(N)} > 0$ ($<$ 0) for $\alpha = 0.5$ (-0.5) and scales as N^2, see Fig. 8(b,e), **as predicted by Eq. (4.11). When $N = \mathcal{O}(1)$, $\lambda_0^{(N)}$ attains its maximal absolute value and decreases to zero as N increases. A numerical fit shows that $\lambda_0^{(N)}$ decays at an exponential rate, see Fig. 8(c,f), consistent with the analytical result $\lambda_0^{(N)} = o(N^{-2})$ of Appendix E. Hence, the numerical simulations suggest that when the beam is centered at a maximum (minimum) of the microstructure, $\lambda_0^{(N)}$ remains positive (negative) also for $N \gg 1$.** Our results for various beam widths are summarized in Table 4.
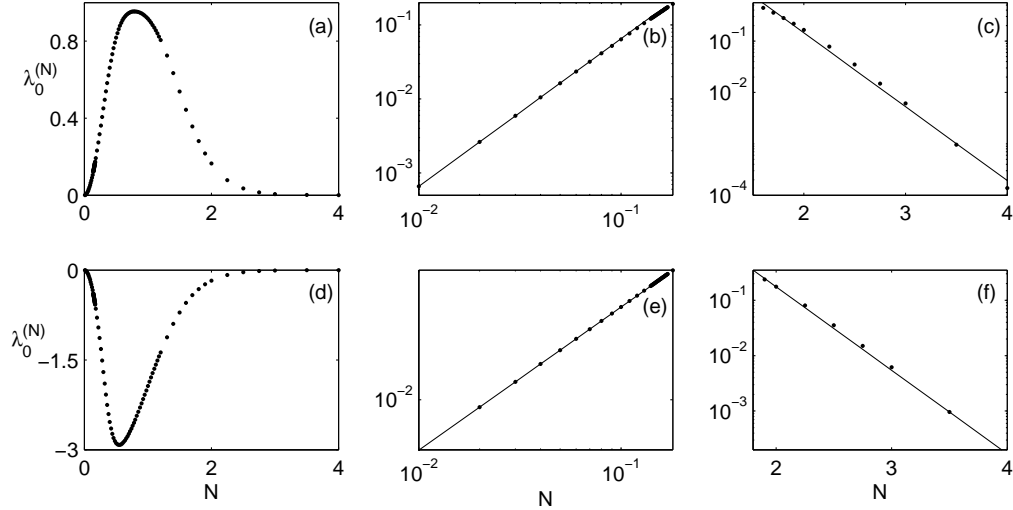

Fig. 8. Eigenvalue $\lambda_0^{(N)}$ of $L_+^{(N)}$ for $p = 5$ as a function of N. The microstructure is $m = \alpha \cos(2\pi Nx)$ with $\alpha = 0.5$ (local maximum; (a) - (c)) and $\alpha = -0.5$ (local minimum; (d) - (f)). (b) and (e): Zoom-in on data of narrow beams ($N \ll 1$). $|\lambda_0^{(N)}|$ is shown on a log-log scale. Solid lines are (b) $6.42N^{1.99}$, (c) $49.4e^{-3.0N}$, (e) $19.7N^{2.00}$, (f) $179.4e^{-3.4N}$.

	Symmetric data		General data	
	local maximum	local minimum	local maximum	local minimum
$N \gg 1$	1	1	probably 1 [a]	probably 2
$N = \mathcal{O}(1)$	1	1	1	2
$N \ll 1$	1	1	1	2

Table 4

$n_-(L_+^{(N)})$, the number of negative eigenvalues of $L_+^{(N)}$, in both the subcritical ($p = 3$) and critical ($p = 5$) cases. Results for $N \gg 1$ in the asymmetric case are based on extrapolation of the numerical observations shown in Fig. 8.

[a] If $p = 3$ and $x = 0$ is a global maximum of $m(Nx)$ then $n_- = 1$, see Section 4.6.1.

4.4 Sign and magnitude of $\partial_\nu \| u^{(N)}(\nu) \|_2^2$

In order to determine the stability of $u_\nu^{(N)}$ by Theorem 10, we need also to calculate the sign $\partial_\nu \| u^{(N)}(\nu) \|_2^2$. Numerical studies suggest that, in addition to the sign of $\partial_\nu \| u^{(N)}(\nu) \|_2^2$, the magnitude of $\partial_\nu \| u^{(N)}(\nu) \|_2^2$ plays an important role in that it determines the size of the stability region. Therefore, in what follows we determine both the sign and magnitude of $\partial_\nu \| u^{(N)}(\nu) \|_2^2$.

4.4.1 Wide bound states ($N \gg 1$)

In the case of wide beams, the sign and magnitude of $\partial_\nu \| u^{(N)}(x, \nu) \|_2^2$ follow from the multiple scales analysis of Section 3.1:

Theorem 19 *Let $u^{(N)}$ be the solution of Eq. (2.11), let $m(X)$ satisfy (2.7) and let $N \gg 1$. Then,*

(1) *$\partial_\nu \| u^{(N)}(\nu) \|_2^2$ is positive for $p < 5$ and negative for $p \geq 5$.*
(2) *The magnitude of $\partial_\nu \| u^{(N)}(\nu) \|_2^2$ is $\mathcal{O}(1)$ when $p \neq 5$ and is $\mathcal{O}(N^{-2})$ when $p = 5$.*

Proof: From Corollary 6 it follows that $\partial_\nu \| u^{(N)}(\nu) \|_2^2 = \partial_\nu \| \mathcal{U}(\nu) \|_2^2 + \mathcal{O}(N^{-2})$. Thus, according to Eq. (4.8) it follows that for $p \neq 5$ the magnitude of the slope is $\mathcal{O}(1)$ and the sign of $\partial_\nu \| u^{(N)}(\nu) \|_2^2$ is the same as in homogeneous medium. When $p = 5$, $\partial_\nu \| \mathcal{U}(\nu) \|_2^2 = 0$ and

$$\partial_\nu \| u^{(N)} \|_2^2 = -\frac{\tau_m}{N^2} \partial_\nu^2 \int \mathcal{U}^{10}(\nu) \, dx + \mathcal{O}(N^{-4}). \tag{4.12}$$

Therefore, $\partial_\nu \| u^{(N)}(\nu) \|_2^2 = \mathcal{O}(N^{-2})$. Differentiating Eq. (3.31) yields

$$\partial_\nu^2 \int \mathcal{U}^{10}(\nu) \; dx = 2\rho_*(5) > 0. \tag{4.13}$$

Substitution in Eq. (4.12) shows that $\partial_\nu \|u^{(N)}(\nu)\|_2^2 < 0$. $\square$.

4.4.2   Narrow bound states ($N \ll 1$)

In the case of narrow beams, the sign and magnitude of $\partial_\nu \|u^{(N)}(x,\nu)\|_2^2$ follow from the perturbation analysis of Section 3.2:

Theorem 20 *Let $u^{(N)}$ be the solution of Eq. (2.11), let $m(Nx) = m(-Nx)$, let $1 + m(0) > 0$ and let $N \ll 1$. Then,*

(1) *$\partial_\nu \|u^{(N)}(x,\nu)\|_2^2$ is positive for $p < 5$ and negative for $p > 5$. When $p = 5$, $\partial_\nu \|u^{(N)}(x;\nu)\|_2^2 > 0$ if and only if $C_{narrow} < 0$ (see Eq. (3.39), i.e., if*

$$\left(1 + m(0)\right) m^{(4)}(0) \; < G_5[m''(0)]^2, \tag{4.14}$$

  where $G_5 \cong -0.3531$ is given by Eq. (3.37).
(2) *The magnitude of $\partial_\nu \|u^{(N)}(x,\nu)\|_2^2$ is $\mathcal{O}(1)$ when $p \neq 5$ and is $\mathcal{O}(N^4)$ when $p = 5$.*

Proof: From Eq. (3.35) it follows that for $p \neq 5$, $\partial_\nu \|u^{(N)}(x,\nu)\|_2^2 = [1 + m(0)]^{\frac{2}{p-1}} \partial_\nu \|\mathcal{U}(x,\nu)\|_2^2 + \mathcal{O}(N^2)$. Therefore, as in the wide beam case, when $p \neq 5$, the microstructure does not alter the sign and changes the magnitude of $\partial_\nu \|u^{(N)}(x,\nu)\|_2^2$ only slightly. When $p = 5$, $\partial_\nu \|\mathcal{U}(x;\nu)\|_2^2 = 0$. Therefore, by Eq. (3.38)

$$\|u^{(N)}(x,\nu)\|_2^2 \approx C_{narrow} \frac{N^4}{\nu^2}. \tag{4.15}$$

Therefore, condition (4.14) follows by direct differentiation and the power slope is $\mathcal{O}(N^4)$ small. $\square$.

Remark 21 *Since $1 + m(0) > 0$ and since $G_5 < 0$, condition (4.14) implies that a necessary condition for a positive slope is $m^{(4)}(0) < 0$.*

4.4.3   Bound states with $N = \mathcal{O}(1)$ width

In order to complete the picture, we use numerical simulations to calculate $\partial_\nu \|u^{(N)}(x,\nu)\|_2^2$ for the four different nonlinear microstructures shown in Fig. 7. Fig. 9 and Fig. 10 show $\|u^{(N)}(x,\nu)\|_2^2$ for $p = 3, 5$ and $N = 1$, as a function of ν. We let ν vary from 0.25 to 4 which, according to Remark 2, correspond to $2 \geq \tilde{N} \geq 0.5$, i.e., beams whose width is $1/2$ to 2 microstructure periods

long. In the subcritical case, the power slope is positive for beams centered at either a local maximum or local minimum. In the critical case, the power slope has $\mathcal{O}(1)$ magnitude and is negative (positive) when centered at a local maximum (minimum) of the microstructure (but see Section 4.5).
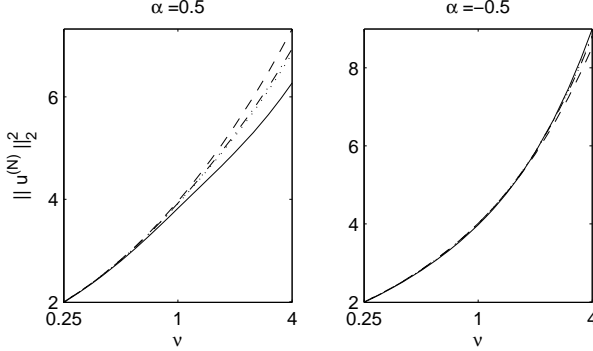

Fig. 9. Power of bound states for the subcritical case $p = 3$ with $\alpha = \pm 0.5$ and $N = 1$ as a function of ν for the microstructures of Fig. 7.
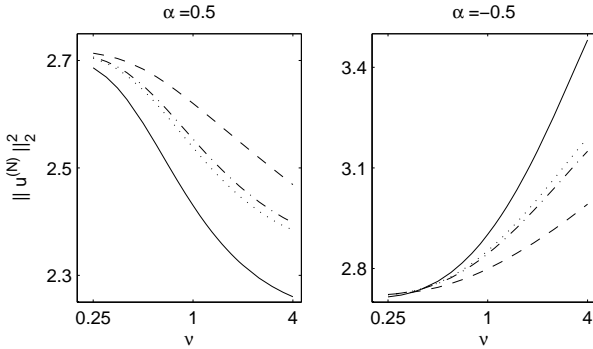

Fig. 10. same as Fig. 9 for the critical case $p = 5$.

4.4.4 Slope condition (S2) - summary

We have seen that in the subcritical case $p = 3$, $\partial_\nu \|u^{(N)}(x,\nu)\|_2^2$ is positive and $\mathcal{O}(1)$ for all beam widths. In Table 5 we summarize the results of Sections 4.4.1-4.4.3 for the critical case ($p = 5$) by showing the sign and magnitude of $\partial_\nu \|u^{(N)}\|_2^2$ for wide, $\mathcal{O}(1)$ and narrow beams centered at either a local maximum or a local minimum of the microstructure. As we have seen, for wide beams ($N >> 1$) $\partial_\nu \|u^{(N)}\|_2^2$ is always negative and is $\mathcal{O}(N^{-2})$. When the beams have $N = \mathcal{O}(1)$ width, $\partial_\nu \|u^{(N)}\|_2^2 = \mathcal{O}(1)$ and its sign is positive for a local minimum and negative for a local maximum. For narrow beams ($N << 1$), $\partial_\nu \|u^{(N)}\|_2^2 = \mathcal{O}(N^4)$ and its sign can be either positive or negative, depending on the values of $m''(0)$ and $m^{(4)}(0)$.

In order to illustrate the results of Table 5, we set $m = \pm 0.5 \cos(2\pi Nx)$ and calculate the power of the bound states for $N = 1$ as ν varies between 0.01

	local maximum	local minimum
$N \gg 1$	$\mathcal{O}(N^{-2})$, negative	
$N = \mathcal{O}(1)$	$\mathcal{O}(1)$, negative	$\mathcal{O}(1)$, positive
$N \ll 1$	$\mathcal{O}(N^4)$, sign determined by Eq. (4.14)	

Table 5
Sign and magnitude of $\partial_\nu \|u^{(N)}\|_2^2$ for wide, $\mathcal{O}(1)$ and narrow bound states centered at a local maximum and minimum of the nonlinear microstructure for the critical case ($p = 5$).

and 30 for the critical case (see Fig. 11). According to Remark 2, these values of ν correspond to $10 = \tilde{N}(\nu = 0.01) \geq \tilde{N} \geq \tilde{N}(\nu = 30) = 0.18$, i.e. to wide, $\mathcal{O}(1)$, and narrow beams. When $\nu \ll 1$ ($\tilde{N} \gg 1$, wide beams) the slope is negative and of $\mathcal{O}(N^{-2})$ magnitude for both curves. The slope is negative (positive) and has $\mathcal{O}(1)$ magnitude for $\mathcal{O}(1)$ beams centered at a local maximum (minimum). For narrow beams, i.e. $\nu \ll 1$ or $\tilde{N} \gg 1$, it can be verified that for $m = \pm 0.5 \cos(2\pi N x)$, condition (4.14) is satisfied only for beams centered at a local minimum so that the slope is negative (positive) for beams centered at a local maximum (minimum). In both cases, the magnitude of the slope is $\mathcal{O}(N^4)$.

Remark 22 *When $\nu \gg 1$ (narrow beams), the local Kerr coefficient at the beam center, $1 + m(0) = 1 + \alpha$, affects the dominant term of the power (see Eq. (3.36)) so the power of the bound state strongly depends on α. However, when $\nu \ll 1$, the dependence on α is only through the $\mathcal{O}(N^{-2})$ correction term (see Eq. (3.1)), hence the two curves are nearly indistinguishable.*
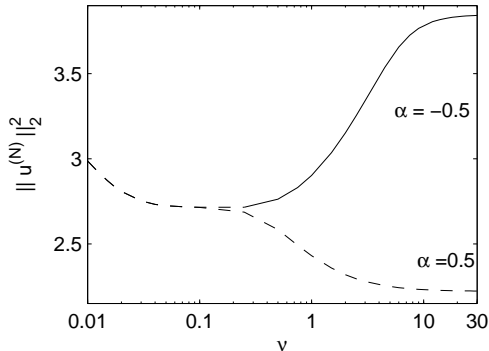

Fig. 11. Power of the bound states as a function of ν for $m = \pm 0.5 \cos(2\pi x)$. Positive slope branch is shown by a solid line and negative slope branches are shown by a dashed line.

4.5 Definition of bound states centered at a local maximum/minimum revisited

We have seen that the stability properties of bound states depend on whether the beam is centered at a local maximum or minimum of the microstructure. The criterion we used for the maximum or minimum was the sign of $m''(0)$. In this Section we show that for $\mathcal{O}(1)$ beams the criterion can be more complex.

We consider the microstructure $m(Nx) = -0.6\cos(2\pi Nx)+0.3\cos(4\pi Nx)$ (see Fig. 12). This microstructure has a shallow local maximum at $x = 0$ with two adjacent global minima. Narrow beams centered at $x = 0$ show the characteristics of beams centered at a local maximum, i.e., that $\lambda_0^{(N)} > 0$, see Fig. 13(a). However, $\mathcal{O}(1)$ beams have the characteristics of $\mathcal{O}(1)$ bound states centered at a local minimum, namely, that $\lambda_0^{(N)} < 0$ (see Fig. 13(a)) and a positive slope (see Fig. 13(b)).

The reason for that is that although the $\mathcal{O}(1)$ beam is centered at a local maximum of the microstructure, the region over which the "bulk of the beam" is centered is of low nonlinear refractive index. Thus, we see that for $\mathcal{O}(1)$ beams, not only the local value of the microstructure at the beam center affects the stability but rather the *area* where the beam is centered (unlike narrow beams which are affected only by the local changes of the microstructure). Henceforth, in order to determine the stability properties of $\mathcal{O}(1)$ beams, one needs to consider the *local* average of the microstructure over the width of the beam. This coarse grained description arises only for microstructures having extrema points which are not global extrema. Hence we did not observe this phenomenon so far when we used the microstructures shown in Fig. 7.
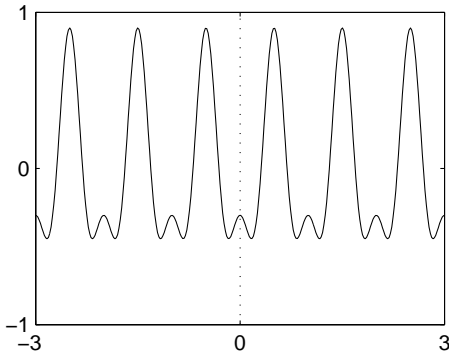

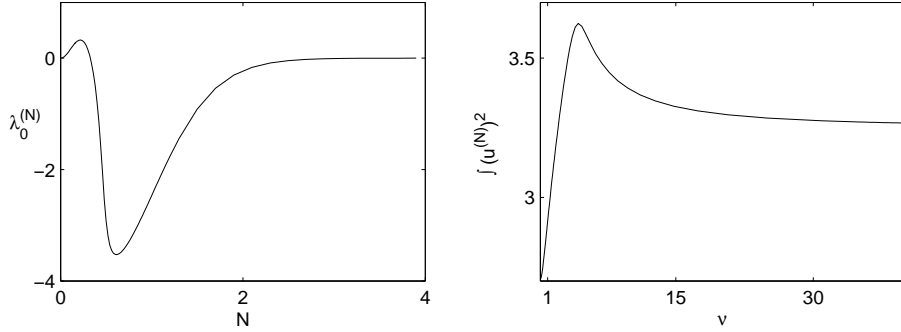Fig. 12. The microstructure $m(Nx) = -0.6\cos(2\pi Nx) + 0.3\cos(4\pi Nx)$ for $N = 1$.

Fig. 13. (a) Eigenvalue $\lambda_0^{(N)}$ of $L_+^{(N)}$ with $\nu = 1$ for the microstructure of Fig. 12. (b) Power of solutions of Eq. (2.11) for the microstructure of Fig. 12 with $N = 1$. Note that $\nu \gg 1$ corresponds to narrow beams and $\nu = \mathcal{O}(1)$ corresponds to $\mathcal{O}(1)$ beams.

4.6 Stability results

At this stage we can combine the results of Theorem 10 concerning the spectral condition (S1) on the number of negative eigenvalues of L_+ (Section 4.3), with our calculations of the slope condition (S2) (Section 4.4). By Theorem 10 these determine the stability or instability of the nonlinear bound state (waveguide) solutions $\phi_{wg} = e^{i\nu z} u^{(N)}$.

4.6.1 Subcritical case $p = 3$

Stability in this case is summarized in Table 1. Since the slope is positive for all beam widths, stability is determined by n_-. As summarized in Table 4, in the symmetric problem $n_- = 1$, hence beams of all widths centered at either a local maximum or minimum of the microstructure are stable. In the asymmetric problem, $n_- = 1$ ($n_- = 2$) for narrow and $\mathcal{O}(1)$ beams centered at a local maximum (minimum) of the microstructure. Thus, narrow and $\mathcal{O}(1)$ beams are stable if centered at a local maximum and unstable if centered at a local minimum.

Since we did not determine the sign of $\lambda_0^{(N)}$ for wide beams, stability of wide beams in the asymmetric case was not determined analytically in this study. In [30], Hajaiej and Stuart proved the stability of the ground state[4] in the asymmetric, subcritical case. Clearly, the ground state is centered at a *global maximum* of the microstructure. Hence, the results of [30] agree with our results for $N \ll 1$ and $N = \mathcal{O}(1)$, and show that wide beams centered at a global maximum are stable. Consequently, we can conclude that in the general problem, $n_- = 1$ for wide beams centered at a global maximum. We note that unlike [30], our stability results apply to bound states centered at any extrema

---

[4] i.e., the bound state with minimal power.

36

of the microstructure, e.g., at a local minimum or even at a local maximum which is not a global one. More importantly, they also apply in the *critical* case.

4.6.2 Critical case $p = 5$

Stability in this case is summarized in Table 2. In the symmetric case $n_-(L_+^{(N)}) = 1$ (see Corollary 17) so that according to Theorem 10, stability is determined by the slope condition. Therefore, when $N \gg 1$ all bound states are unstable. Beams of $\mathcal{O}(1)$ width which are centered at a local minimum (maximum) are stable (unstable) and narrow beams are stable if and only if condition (4.14) is satisfied[5]. We recall that the slope magnitude for narrow beams is much smaller ($\mathcal{O}(N^4)$) than for $\mathcal{O}(1)$ beams ($\mathcal{O}(1)$ slope). Thus, stability of narrow beams is expected to be much weaker than for $\mathcal{O}(1)$ beams.

In the asymmetric problem, when $N \gg 1$, the negative slope of $\|u^{(N)}(\nu)\|_2^2$ implies that these solutions are unstable regardless of the (unknown) sign of $\lambda_0^{(N)}$. $\mathcal{O}(1)$ beams satisfy $n_-(L_+^{(N)}) = 1$ only when centered at a local maximum. In this case the slope is negative so that these beams are unstable. Therefore, in the general problem, beams can be stable only if they have $N \ll 1$ width and if centered at a local maximum of a microstructure that satisfies condition (4.14). Even then, since the slope magnitude is $\mathcal{O}(N^4)$, we expect the stabilization induced by the microstructure to be extremely weak.

4.7 The spectral condition (S1) revisited

In Section 4.3, we have seen that $n_- = 2$ in the general problem (4.10) when the beam is centered at a local minimum of the microstructure. Hence, this bound state is always unstable. However, $n_- = 1$, (hence, beams can be stable) when the bound state is centered at a local maximum. In order to motivate this finding, we look at the transverse velocity and acceleration of the beam center of mass, defined as

$$\langle x \rangle = \frac{\int x|\phi|^2}{\int |\phi|^2} = \frac{\int x|\phi|^2}{\int |\phi_0|^2}. \tag{4.16}$$

Proposition 23 *Let ϕ be a solution of Eq. (2.4). Then,*

---

[5] In [21] Fibich and Wang used a rigorous variational approach to study ground states of (2.4) for the d-dimensional symmetric problem with $N \ll 1$ and $d \geq 2$. They derive a condition for stability which is a generalization of condition (4.14) to multi-dimensions.

$$\frac{d}{dz} \int x|\phi|^2 \ dx = 2 \ Im \int \phi_x \phi^* \ dx, \tag{4.17}$$

and

$$\frac{d^2}{dz^2} \int x|\phi|^2 \ dx = \frac{4N}{p+1} \int m'(Nx)|\phi|^{p+1} \ dx. \tag{4.18}$$

Proof: Differentiate the right-hand-sides with respect to z, use Eq. (2.4) and integrate by parts.

Let us perturb the beam center by considering the initial condition $\phi_0 = u^{(N)}(x - \delta_c)$ where $u^{(N)}$ is the solution of Eq. (2.11). From Proposition 23 it follows that

$$\left. \frac{d \langle x \rangle}{dz} \right|_{z=0} = 0,$$

i.e., the initial lateral velocity of the beam center is zero for $\phi_0 = u^{(N)}(x - \delta)$. Calculation of the initial lateral acceleration leads to the following result:

Corollary 24 *Narrow bound states that are centered slightly off a local extremum of the microstructure have an initial acceleration towards the nearest local maximum of the microstructure.*

Proof: See Appendix F.

Thus, the instability of beams centered at a local minimum of the microstructure stems from their attraction to regions with higher Kerr nonlinearity. This explains why such beams can be stable in the symmetric problem (which does not allow lateral perturbations), and also why in the asymmetric case, for both the subcritical and critical cases, beams centered at a local minimum of the microstructure are unstable.

The instability of bound states centered at a local minimum of the microstructure under asymmetric perturbations was observed also in discrete [?] and continuous [?] *linear* microstructures. In the discrete model, instability of bound states centered between the waveguides (i.e., at a local minimum of the linear microstructure) is attributed to the Peierls-Nabarro potential [40], an effective potential that increases the Hamiltonian of beams centered at a local minimum of the linear microstructure with respect to beams centered at a local maximum with the same power. In that sense, the cases of linear and nonlinear microstructures are similar since for a fixed state, centering it about a local maximum (minimum) of $m(Nx)$ appears to be the best choice for minimizing (maximizing) the energy functional $\mathcal{E}_\nu$, see (4.4), as it would make the second term in $\mathcal{H}$ most negative (positive), while the first term in $\mathcal{H}$ and $\mathcal{P}$ are independent of the centering. Hence, one expects instability of states centered

38

at a local minimum of $m(Nx)$, and provided $\mathcal{H}$ is bounded below for fixed $\mathcal{P}$, stability of states with their maximum centered about a local maximum of $m(Nx)$.

5 Stability of bound states - Simulations

In this section we consider the stability of the nonlinear bound state $\phi_{wg} = e^{iz}u^{(N)}(x; \nu = 1)$. We show the dynamics of bound states and especially the different types of instabilities that can develop in various cases. We solve Eq. (2.4) numerically using a fourth-order implicit finite-difference scheme with the initial condition

$$\phi(x,0) = (1 + \delta_p)u^{(N)}(x - \delta_c; \nu = 1).$$

Thus, δ_p perturbs the power of the bound state but preserves its symmetry with respect to $x = 0$, and δ_c shifts the beam center from $x = 0$ to $x = \delta_c$ but preserves its power. **The values of dz and dx were chosen to ensure grid convergence. In the symmetric case, we solved Eq. (2.4) only for $0 < x < \infty$ and used the boundary condition $\partial_x\, u^{(N)}(0) = 0$. The full solution was obtained by reflection about $x = 0$. In the general asymmetric case, we solved Eq. (2.4) for $-\infty < x < \infty$.**

Instead of presenting the H^1 difference between the solution ϕ and the waveguide solution ϕ_{wg}, we plot the maximal amplitude of the solution after verifying that the dynamics of the difference between the maximal amplitude and the initial maximal amplitude is qualitatively similar to the dynamics of the H^1 difference. The advantage of this approach is that in addition to stability, the maximal amplitude also provides information on the character of the dynamics in the stable and unstable cases, *e.g.* blow-up, diffraction, *etc.*). We also present the dynamics of the center of mass of the beam (defined in Eq. (4.16)). Together, these two quantities give a fairly comprehensive description of the dynamics.

5.1 Subcritical case $p = 3$

We first consider $N = \mathcal{O}(1)$ beams centered at a local maximum of the microstructure. In these simulations and those that follow, the microstructure is given by $m(Nx) = \alpha\cos(2\pi Nx)$. In the symmetric case ($\delta_c = 0$, Fig. 14(a)), a perturbation of the power induces only small oscillations of the maximal amplitude. Similarly, a small lateral shift of the incident beam ($\delta_c \neq 0$ and $\delta_p = 0$) results in small oscillations of the beam center about the local maximum of

the microstructure while hardly affecting the maximal amplitude (Fig. 14(b)). Combining the two perturbations results in simultaneous small oscillations of the maximal amplitude and beam center (Fig. 14(c)). Thus, we see that $\mathcal{O}(1)$ beams centered at a local maximum are stable under arbitrary (symmetric and asymmetric) perturbations; see Table 1.
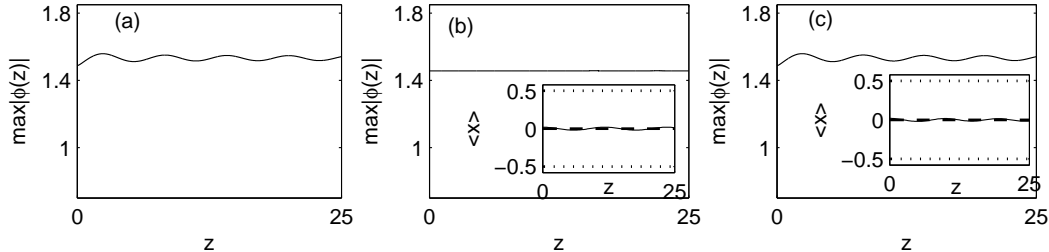

Fig. 14. Maximal amplitude of solutions of Eq. (2.4) for $p = 3$, $N = 1$, $\alpha = 0.5$. (a) $\delta_p = 0.02$ and $\delta_c = 0$. (b) $\delta_p = 0$ and $\delta_c = 0.02$. The inset shows the position of the beam center of mass (solid line) with respect to the local maximum (dashed line) and local minima (dotted line) of the microstructure. (c) Similar to (b) with $\delta_c = 0.02$ and $\delta_p = 0.02$.

Dynamics of $\mathcal{O}(1)$ beams centered at a local minimum of the microstructure is qualitatively similar to beams centered at a local maximum as long as the symmetry is maintained (Fig. 15(a)). However, a lateral shift of the incident beam results in a large drift of the beam center towards the nearest maximum of the microstructure and oscillations about it together with $\mathcal{O}(1)$ oscillation of the maximal amplitude (Fig. 15(b)). Unlike the stable beams centered at a local maximum, the drift increases rather than decreases as $\delta_c \to 0$. This is to be expected, because smaller δ_c with respect to a local minimum is, in effect, a larger perturbation with respect to the nearest local maximum. Adding a perturbation to the power (Fig. 14(c)) does not alter the dynamics significantly. Thus, we conclude that beams centered at a local minimum are stable in the symmetric case but unstable in the general problem, in agreement with Table 1. The dynamics of wide and narrow beams are qualitatively similar (data not shown).

5.2   Critical case $p = 5$

We first consider $\mathcal{O}(1)$ beams centered at a local maximum of the microstructure. A slight increase in the beam power ($\delta_p > 0$) results in a finite-distance collapse; see Fig. 16(a). In addition, when the beam center is shifted from the local maximum it no longer has enough power for blow-up and thus, it diffracts; see Fig. 16(b). The dynamics of wide beams centered at a local maximum is qualitatively similar (data not shown). Thus, as summarized in Table 2, wide and $\mathcal{O}(1)$ beams centered at a local maximum are unstable. We also note that this instability is similar to one in homogeneous Kerr medium,
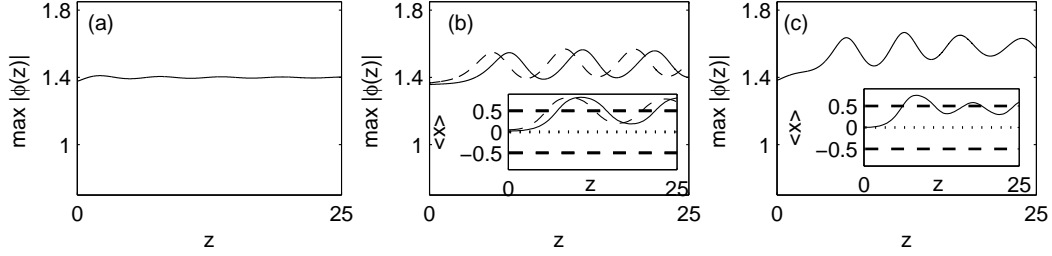
Fig. 15. Maximal amplitude of solutions of Eq. (2.4) for $p = 3$, $N = 1$, $\alpha = -0.5$. (a) $\delta_p = 0.02$ and $\delta_c = 0$. (b) $\delta_p = 0$ and $\delta_c = 0.02$ (solid line) and $\delta_c = 0.05$ (dashed line). The inset shows the position of the beam center of mass (solid line) with respect to the local maximum (dashed line) and local minima (dotted line) of the microstructure. (c) Similar to (b) with $\delta_c = 0.02$ and $\delta_p = 0.02$.

i.e., the beam either develops a self-focusing singularity (blows up) or diffracts to zero [54].
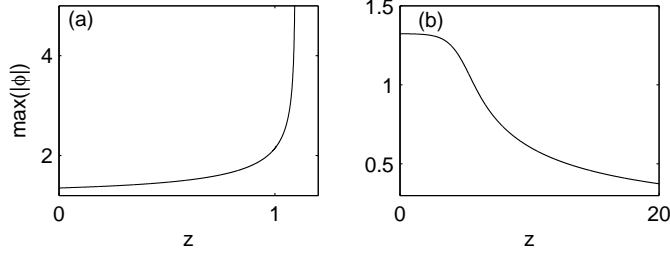

Fig. 16. Maximal amplitude of solutions of Eq. (2.4) for $p = 5$, $N = 1$, $\alpha = 0.5$. (a) $\delta_p = 0.02$ and $\delta_c = 0$. (b) $\delta_p = 0$ and $\delta_c = 0.02$.

In Fig. 17 we show the dynamics of $\mathcal{O}(1)$ beams centered at a local minimum of the microstructure. In Table 2, in the symmetric problem, these beams are stable since as $\delta_p \to 0$, the oscillations become smaller (Fig. 17(a)). In contrast, a small shift of the initial beam center causes it to drift toward the nearest maximum and, consequently, to blow-up; see Fig. 17(b). Perturbing both the power and beam center only accelerates the blow-up; see Fig. 17(c). We note that the generic location of the singularity is not at the local maximum of the microstructure. Indeed, in Fig. 18 we show that the blowup point (which is different from the center of mass) of the beam shown in Fig. 17(b) is beyond the nearest local maximum. Note that an input beam with the same lateral shift but with higher input power blows up before the local maximum. These simulations show that $\mathcal{O}(1)$ beams are stable in the symmetric case but unstable in the asymmetric case, in agreement with Table 2.

In Fig. 19(a) we show that in the symmetric case, wide beams centered at a local minimum whose power is slightly above the power of the bound state ($\delta_p > 0$) undergo self-focusing but do not blow-up. The reason for that is that after the initial focusing, the beams reach an $\mathcal{O}(1)$ width where they become stable; see Fig. 17(a). Despite the arrest of collapse, these wide beams
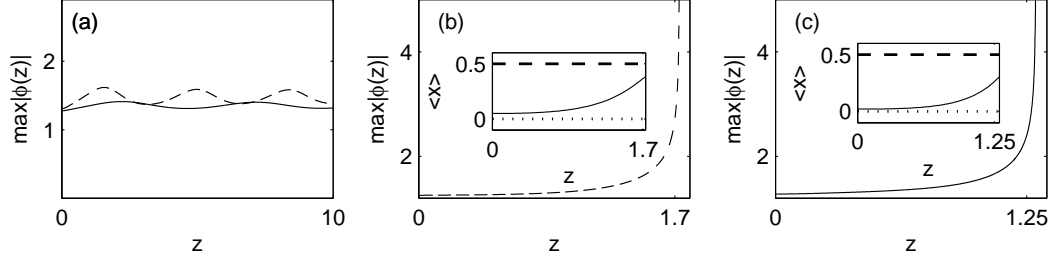
41

Fig. 17. Maximal amplitude of solutions of Eq. (2.4) for $p = 5$, $N = 1$, $\alpha = -0.5$. (a) $\delta_p = 0.02$ (dashed line), $\delta_p = 0.05$ (solid line) and $\delta_c = 0$. (b) $\delta_p = 0$ and $\delta_c = 0.02$. The inset shows the position of the beam center of mass (solid line) with respect to the local maximum (dashed line) and local minimum (dotted line) of the microstructure. (c) Similar to (b) with $\delta_c = 0.02$ and $\delta_p = 0.02$.
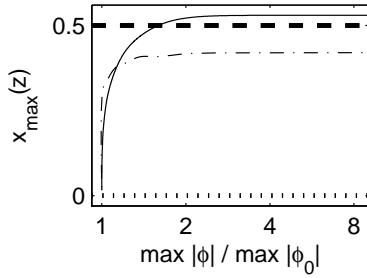

Fig. 18. Location of maximal amplitude $(x_{max}(z))$ as a function of focusing level for solutions of Eq. (2.4) for $p = 5$, $N = 1$, $\alpha = -0.5$, $\delta_c = 0.02$, $\delta_p = 0$ (solid line) and $\delta_p = 0.5$ (dashed-dotted line). Local maximum and minimum of the microstructure are shown by a dashed line and a dotted line, respectively.

are unstable as smaller perturbation only delays the self-focusing but does not reduce its magnitude. We note that this instability is different from the typical blowup/ diffraction instability of the homogeneous NLS. Of course, any symmetry breaking in the initial condition (e.g., $\delta_c \neq 0$ or even random noise) would result in a drift instability, i.e., a shift to the nearest maximum of the microstructure and to collapse, similar to Fig. 17(b,c).
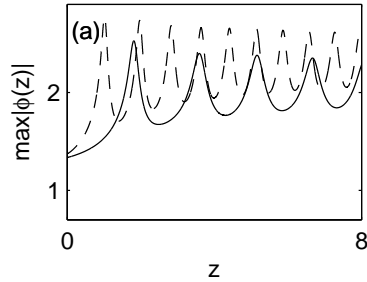

Fig. 19. Maximal amplitude of solutions of Eq. (2.4) for $p = 5$, $N = 4$, $\alpha = -0.5$, $\delta_c = 0$ and $\delta_p = 0.02$ (solid line), $\delta_p = 0.05$ (dashed line).

In the general, asymmetric critical case, the only stable bound states are narrow beams centered at a local maximum of microstructures that satisfy con-

dition (4.14); see Table 2. Since the microstructure $m = \alpha \cos(2\pi N x)$ satisfies condition (4.14) only for beams centered at a local minimum, we use the microstructure $m = 0.48 \cos(2\pi N x) - 0.1 \cos(4\pi N x)$ for which beams centered at a local maximum do satisfy condition (4.14). In the symmetric problem, narrow beams of this microstructure are indeed stable under $\mathcal{O}(10^{-4})$ perturbations, as can be seen in Fig. 20(a). However, since perturbations as small as $\delta_p = 0.01$ result in blowup, the stability region is extremely small (compare, for instance, with Fig. 17(a)). The smallness of the stability region is attributed to the $\mathcal{O}(N^4)$ small slope of the power curve, see Eq. (3.36). Fig. 20(b) shows that the beam is also stable under asymmetric perturbations (which do not have to be as small). The stability with respect to such perturbations is attributed to the $\mathcal{O}(N^2)$ positive value of the eigenvalue $\lambda_0^{(N)}$ (see Eq. (4.11)). Finally, stability is maintained if we simultaneously perturb the power and lateral position (see Fig. 20(c)).

The dependence of stability on the properties of the microstructure through condition (4.14) is further demonstrated in Fig. 21, where we solve Eq. (2.4) for the one-parameter family of microstructures $m(Nx) = 0.48 \cos(2\pi N x) - \gamma \cos(4\pi N x)$ for which the $\partial_\nu \int [u^{(N)}]^2$ is positive (negative) for $\gamma > \gamma_c$ ($\gamma < \gamma_c$) where $\gamma_c \cong 0.032$. Indeed, for the given perturbation $\delta_p = 10^{-4}$, $\delta_c = 0$, the solution blows up for $\gamma = 0.03$ and is stable for $\gamma = 0.1$ and $\gamma = 0.075$. The "unexpected" blowup at $\gamma = 0.05$ is due to the very small slope $\left(\partial_\nu \int \left(u^{(N)}\right)^2 \cong 0.0025\right.$ at $\gamma = 0.05$) that implies a very small stability region. Indeed, we confirmed that the beam is "mathematically stable" at $\gamma = 0.05$, i.e., that under a smaller perturbation $\delta_p = 4 \cdot 10^{-5}$ the beam is stable (data not shown).
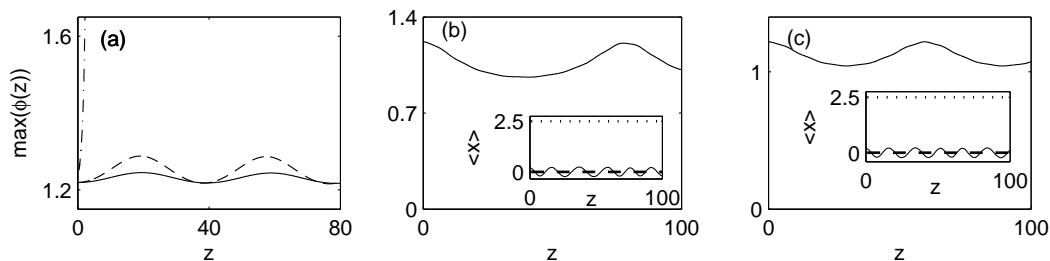

Fig. 20. Maximal amplitude of solutions of Eq. (2.4) with the microstructure $m = 0.48 \cos(2\pi N x) - 0.1 \cos(4\pi N x)$ for $p = 5$ and $N = 0.2$. (a) $\delta_c = 0$ and $\delta_p = 4 \cdot 10^{-5}$ (solid line), $\delta_p = 10^{-4}$ (dashed line) and $\delta_p = 0.01$ (dash-dotted line). (b) $\delta_p = 0$ and $\delta_c = 0.2$. The inset shows the position of the beam center of mass with respect to the local maximum (dashed line) and local minimum (dotted line) of the microstructure. (c) Similar to (b) with $\delta_c = 0.2$ and $\delta_p = 10^{-4}$.
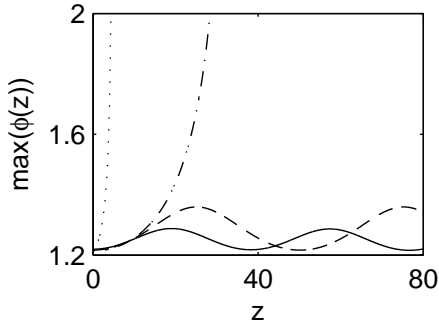
Fig. 21. Maximal amplitude of solutions of Eq. (2.4) with the microstructure $m = 0.48 \cos(2\pi Nx) - \gamma \cos(4\pi Nx)$ for $p = 5$, $\delta_p = 10^{-4}$, $\delta_c = 0$, and $N = 0.2$. $\gamma = 0.1$ (solid line), $\gamma = 0.075$ (dashed line), $\gamma = 0.05$ (dash-dotted line), $\gamma = 0.03$ (dotted line).

6 Summary and discussion

In this paper we have used a combination of rigorous analysis, asymptotic analysis, and numerical simulations to study the structure and dynamic stability properties of bound states of the scalar one-dimensional NLS with a transverse periodic nonlinear microstructure and general p^{th} power nonlinearity, Eq. (1.7). We chose the one-dimensional model to simplify the presentation; the general multi-dimensional problem can be treated by a natural extension of the methods presented herein. In particular, the critical case $p = 5$ is mathematically analogous to the important case of Kerr nonlinearity $p = 3$ in spatial dimension $d = 2$ [**?**].

Some of the results obtained in this paper can be obtained using Evans function methods; see, for example, [34]. These methods are particularly well suited to one space-dimensional problems. Note, however, that the methods we use in this paper (multiple scale / homogenization expansions, perturbation theory of spectra and variational methods) are not specific to one dimensional analysis, and can naturally be extended to multi-dimensional cases.

We introduce and emphasize the importance of the dimensionless parameter $N = r_{\text{beam}}/r_{\text{ms}}$, the ratio of beam width to the microstructure period. Our study appears to be the first wherein the three regimes: wide ($N \gg 1$), narrow ($N \ll 1$) and intermediate ($N = \mathcal{O}(1)$) beams are systematically considered. Moreover, to the best of our knowledge, this is the first *analytic* study of *wide* beams in a microstructured media. The problem of stability at different beam width regimes are, in fact, interconnected; the width of an unstable beam can change significantly with propagation. For example, we observe that in the symmetric case, a bound state centered at a microstructure minimum is unstable if the beam is wide but stable if the bound state is $O(1)$. There-

44

fore, when an unstable wide bound state self-focuses to one of $\mathcal{O}(1)$ width, it becomes stabilized.

Theorem 10 asserts that a nonlinear bound state is orbitally stable if and only if the spectral condition, (S1), ($n_-(L_+) \leq 1$) and the slope condition, (S2), ($\partial_\nu \|u\|_2^2 > 0$) hold. These conditions together imply that a state $u^{(N)}$ is a local minimizer of $\mathcal{H}$ subject to fixed $\mathcal{P}$. Very roughly speaking, if the slope condition, (S2), is violated then either nonlinearity dominates diffraction or vice versa. Hence, the bound state becomes unstable either by collapsing or by diffractively spreading and approaching zero. This *blowup/diffraction instability* scenario, studied in the homogeneous case for NLS at criticality ($p = 1 + 4/d$) [54], is supported by our numerical studies. We have also numerically studied the situation where the spectral condition (S1) does not hold, but the slope condition, (S2), holds. This results in a *drift instability*, as exhibited by the formal Ehrenfest-type computation in Section 4.7, which is excited only by asymmetric perturbations. The importance of the spectral condition is demonstrated by the occurrence of a drift instability even when the power slope is positive. Although previous studies have already demonstrated instability when the slope condition is satisfied (but the spectral condition is not), see *e.g.*, [42], in numerous other studies the importance of the spectral condition was overlooked and only the slope condition was tested for determining stability.

We have shown analytically that in the critical case $p = 5$, a nonlinear microstructure can stabilize the beam only in the case of a narrow beam which is centered at a local maximum of a microstructure that satisfies condition (4.14). Our simulations revealed that these bound states are indeed stable, but only relative to extremely small perturbations. Therefore, it seems likely that nonlinear microstructure by itself cannot stabilize a laser beam since typically, in actual physical setups the profile of the incident beam can be controlled up to a few percent accuracy. Thus, it may be that the bound state of Fig. 20 is mathematically stable but physically unstable. As noted, the extreme smallness of the basin of stability about that bound state appears related to the $\mathcal{O}(N^4)$ small slope of the curve $\nu \mapsto \partial_\nu \|u^{(N)}\|_2^2$. Further research is needed to establish the relation between the magnitude of the (positive) slope and the size of the basin of stability.

Finally, we believe that some of the analytical contributions of this study, namely,

(1) the identification of the importance of the beam width parameter,
(2) the multiple scales analysis for calculation of wide beams,
(3) the perturbation analysis for calculation of narrow beams (which was first

done in [21])

(4) the realization that in the case of "physical stability" there is a "third condition" that involves the magnitude of the slope, which determines the size of the stability region,

may prove useful in other settings where equations of nonlinear Schrödinger equation type with spatially varying coefficients arise.

Acknowledgements

A   Proof of Corollary 6

By Theorem 3,

$$
\begin{aligned}
\|u^{(N)}\|_2^2 &= \|\mathcal{U}\|_2^2 \;+\; \frac{2p}{N^2}\; \tau_m \int \mathcal{U}\, L_+^{-1}[\mathcal{U}^{2p-1}] \;+\; \mathcal{O}(N^{-4}) \qquad\qquad \text{(A.1)}\\
&= \|\mathcal{U}\|_2^2 \;+\; \frac{1}{N^2}\; \tau_m \int 2p\mathcal{U}^{2p-1}\, L_+^{-1}[\mathcal{U}] \;+\; \mathcal{O}(N^{-4}).
\end{aligned}
$$

We note that there is a $\mathcal{O}(N^{-2})$ "cross-term" in Eq. (A.1)

$$
-\frac{2}{N^2} \int \mathcal{U}(x,\nu)^{p+1}\, \partial_X^{-2} m(Nx)\; dx,
$$

which we have neglected. We claim that if $m(X)$ is at least piecewise continuous, this term is of order $N^{-2}\exp(-\kappa N)$. Since $m(X)$ is periodic, it has the Fourier expansion

$$
m(X) \;=\; \sum_{|k|\geq 1} m_k e^{2\pi i k X}.
$$

In the worst case where m has jump discontinuities, $m_k = \mathcal{O}(|k|^{-1})$ for large k. Also,

$$
\partial_X^{-2} m(Nx) \;=\; \sum_{|k|\geq 1} (2\pi i k)^{-2}\; m_k e^{2\pi i k N x},
$$

The cross-term (A.2) is then controlled by

$$
\frac{1}{N^2} \sum_{|k|\geq 1} \frac{1}{k^2}\, m_k \int \mathcal{U}(x,\nu)^{p+1}\; e^{2\pi i k N x}\; dx.
$$

Since $\mathcal{U}$ is analytic in a strip about the real axis, the previous expression is bounded by

$$\frac{C}{N^2} \sum_{|k| \geq 1} \frac{1}{k^3} e^{-\kappa |k| N} \leq \frac{C}{N^2} e^{-\kappa N}, \quad \kappa > 0.$$

In order to proceed, we use the following Lemma:

Proposition 25 *Let $\mathcal{U}$ and L_+ be given by Eq. (2.10) and Eq. (3.3). Then, $\partial_\nu \mathcal{U} = -L_+^{-1} \mathcal{U}$.*

Proof: Differentiating Eq. (2.9) with respect to ν gives

$$0 = \partial_\nu \left(\partial_x^2 \mathcal{U} \right) + \partial_\nu \, \mathcal{U}^p - \partial_\nu \, (\nu \mathcal{U}) = \partial_x^2 \left(\partial_\nu \mathcal{U} \right) + p \mathcal{U}^{p-1} \left(\partial_\nu \mathcal{U} \right) - \mathcal{U} - \nu \partial_\nu \mathcal{U} =$$
$$= -L_+ \partial_\nu \mathcal{U} - \mathcal{U}.$$

$\square$.

Using Proposition 25 in Eq. (A.1) gives

$$\|u^{(N)}\|_2^2 = \|\mathcal{U}\|_2^2 - \frac{1}{N^2} \, \tau_m \int \partial_\nu \mathcal{U} \, 2p \mathcal{U}^{2p-1} + \, \mathcal{O}(N^{-4})$$
$$= \|\mathcal{U}\|_2^2 - \frac{1}{N^2} \, \tau_m \partial_\nu \int \mathcal{U}^{2p} \, dx + \, \mathcal{O}(N^{-4}),$$

which proves Corollary 6.

B   Numerical computation of bound states by the spectral renormalization method

The numerical method that we use to calculate bound states was first introduced by Petviashvili [44] and more recently by Ablowitz, Musslimani and co-workers in a series of papers [2,4,6,41]; for a recent review, see [5]. Here, we derive the method using a different approach which, we believe, makes it somewhat more intuitive.

Let u_V be the nontrivial solution of

$$-\partial_x^2 u(x) - V(x)|u|^{p-1} u + \nu u = 0, \tag{B.1}$$

and let $\mathcal{F}(u) = \int_{-\infty}^{\infty} u(x) e^{-ikx} dx$ be the Fourier transform of u. Taking the Fourier transform of Eq. (B.1) and rearranging yields

$$\mathcal{F}(u) = \frac{1}{k^2 + \nu} \mathcal{F}(V(x)|u|^{p-1} u).$$

This equation can be solved with the fixed point iterations

$$\mathcal{F}(u_{m+1}) = \frac{1}{k^2 + \nu} \, \mathcal{F}(V(x)|u_m|^{p-1}u_m), \qquad m = 0, 1, \ldots \qquad \text{(B.2)}$$

so that $u_{m+1} = \mathcal{F}^{-1}\left(\frac{1}{k^2+\nu} \, \mathcal{F}(V(x)|u_m|^{p-1}u_m)\right)$. Unfortunately, numerical simulations show that the iterations (B.2) usually converge to the fixed points $u_\infty \equiv 0$ or $u_\infty \equiv \infty$, rather than to u_V. This divergence can be understood in the following way. Suppose, for example, that at some stage in the iterations we have $u_m = Cu_V$ where C is a complex constant. In this case,

$$\mathcal{F}(u_{m+1}) = \frac{1}{k^2 + \nu} \, \mathcal{F}(V(x)C^{p-1}|u_V|^{p-1} \, Cu_V) \equiv C^p \mathcal{F}(u_V),$$

i.e., $u_{m+1} = C^p u_V$. Therefore, the iterations will diverge to $u_\infty \equiv 0$ if $|C| < 1$ and to $u_\infty \equiv \infty$ if $|C| > 1$.

The argument above shows that in order to make sure that the iterations converge to u_V, we need somehow to prevent the L_2 norm of u_m from going to zero or to infinity. To do that, we multiply Eq. (B.2) by $\left[\mathcal{F}(u)\right]^*$ and integrate over k, resulting in the integral identity

$$\int |\mathcal{F}(u)|^2 dk = \int \frac{1}{k^2 + \nu} \mathcal{F}(V(x)|u|^{p-1}u)\left[\mathcal{F}(u)\right]^* dk. \qquad \text{(B.3)}$$

In general, u_m does not satisfy condition (B.3). Therefore, we define $u_{m+\frac{1}{2}} = C_m u_m$ where the real constant C_m is chosen so that $u_{m+\frac{1}{2}}$ will satisfy identity (B.3). Specifically, let

$$\text{SL}_m \equiv \int |\mathcal{F}(u_m)|^2 dk, \qquad \text{SR}_m \equiv \int \frac{1}{k^2 + \nu} \mathcal{F}(V(x)|u_m|^{p-1}u_m)\left[\mathcal{F}(u_m)\right]^* dk.$$

Therefore, the real constant C_m is chosen so that $C_m^2 \, \text{SL}_m = C_m^{p+1} \, \text{SR}_m$. This equation has three solutions: $C_m = 0$ (corresponding to $u_\infty = 0$), $C_m = \infty$ (corresponding to $u_\infty = \infty$) and the nontrivial solution

$$C_m = \left(\frac{\text{SL}_m}{\text{SR}_m}\right)^{\frac{1}{p-1}}, \qquad \text{(B.4)}$$

corresponding to $u_\infty = u_V$. Therefore, we can avoid the divergence to $u_\infty = \infty$ or $u_\infty = 0$ by applying the iterations (B.2) to $u_{m+\frac{1}{2}}$ instead of u_m, i.e.,

$$\mathcal{F}(u_{m+1}) = \left(\frac{\text{SL}_m}{\text{SR}_m}\right)^{\frac{p}{p-1}} \frac{1}{k^2 + \nu} \mathcal{F}(V(x)|u_m|^{p-1}u_m). \qquad \text{(B.5)}$$

The idea that the iterations (B.2) can be made to converge by adding the multiplication by the $(SL/SR)^{p/p-1}$ term was derived in [5] from a "homoge-

nization" [6] argument. We believe that our derivation is more intuitive since it shows that by choosing C_m as in (B.4), we restrict the iterations to the family of solutions $\{u|\ u$ satisfies (B.3), $u \not\equiv 0,\ u \not\equiv \infty\}$.

In this paper we are interested in solutions of Eq. (B.1) with $V(x) = 1 + m(Nx)$ where m is a periodic function, e.g., $m = \alpha\cos(2\pi Nx)$. These solutions are centered at $x = 0$, which is a local maximum (minimum) of the microstructure for $\alpha > 0$ ($\alpha < 0$). Since if $u(x)$ is even and real then $\mathcal{F}(u)$ is also even and real, if we choose the initial guess u_0 to be even and real, then u_m should remain even and real for all m. However, in our simulations we found out that in some cases, numerical roundoff errors lead to the accumulation of an imaginary component of u_m that eventually shift the center of the solution away from $x = 0$. For example, an initial guess centered at a local minimum might converge to a solution centered at a local maximum. In order to avoid this undesirable effect due to the accumulation of the imaginary component, we added the stage $u_m \to |u_m|$, i.e.,

$$u_{m+1} = \left| \mathcal{F}^{-1}\left(\left(\frac{SL_m}{SR_m}\right)^{\frac{p}{p-1}} \frac{1}{k^2 + \nu}\ \mathcal{F}(V(x)|u_m|^{p-1}u_m) \right) \right|.$$

We note that the trick $u_m \to |u_m|$ works because the ground state of a second order elliptic problem is of one sign.

C   Perturbation analysis for $N \ll 1$

In this Appendix, we use a perturbation analysis to solve Eq. (2.11) for narrow beams. The derivation follows the same lines as [21]. We define $u^{(N)}(x) = \left(\frac{1}{1+m(0)}\right)^{\frac{1}{p-1}} S(x)$. Then, the equation for S is

$$-\partial_x^2 S - \frac{1 + m(Nx)}{1 + m(0)}S^p + \nu S = 0. \tag{C.1}$$

Taylor expansion of the microstructure gives

$$\frac{1 + m(Nx)}{1 + m(0)} = 1 + aN^2x^2 + bN^4x^4 + \mathcal{O}(N^6), \tag{C.2}$$

where $a = m''(0)/2[1 + m(0)]$ and $b = m^{(4)}(0)/24[1 + m(0)]$. We look for a solution of Eq. (C.1) of the form

$$S = \mathcal{U} + N^2g(x) + N^4h(x) + \mathcal{O}(N^6), \tag{C.3}$$

---

[6] The meaning of the term "homogenization" in [5] is obviously different from the one we use in the main body of this paper.

where $\mathcal{U}$ is given by Eq. (2.10). Therefore,

$$S^m = \mathcal{U}^m + N^2 m \mathcal{U}^{m-1} g + N^4 \left(m \mathcal{U}^{m-1} h + \binom{m}{2} \mathcal{U}^{m-2} g^2 \right) + \mathcal{O}(N^6),$$

and the equations for g and h are

$$-L_+ g = -a\, x^2 \mathcal{U}^p, \tag{C.4}$$

$$-L_+ h = -\binom{p}{2} \mathcal{U}^{p-2} g^2 - b\, x^4 \mathcal{U}^p - a\, p\, x^2\, \mathcal{U}^{p-1} g,$$

where L_+ is defined in (3.3). We multiply Eq. (2.9) by S, use the ansatz (C.3) and integrate. Collecting the $\mathcal{O}(N^2)$ and $\mathcal{O}(N^4)$ terms gives

$$\int \mathcal{U}_x\, g_x + \nu \int \mathcal{U} g - \int \mathcal{U}^p\, g = 0, \tag{C.5}$$

and

$$\int \mathcal{U}_x\, h_x + \nu \int \mathcal{U} h - \int \mathcal{U}^p\, h = 0, \tag{C.6}$$

respectively. We multiply Eq. (C.1) by $\mathcal{U}$, use ansatz (C.3) and integrate. Collecting the $\mathcal{O}(N^2)$ and $\mathcal{O}(N^4)$ terms gives

$$\int \mathcal{U}_x\, g_x + \nu \int \mathcal{U} g - p \int \mathcal{U}^p\, g = a \int x^2 \mathcal{U}^{p+1}, \tag{C.7}$$

$$\int \mathcal{U}_x\, h_x + \nu \int \mathcal{U} h - p \int \mathcal{U}^p\, h - \binom{p}{2} \int \mathcal{U}^{p-1} g^2 - a\, p \int x^2 \mathcal{U}^p g$$

$$= b \int x^4 \mathcal{U}^{p+1}. \tag{C.8}$$

Next we derive the *Pohozaev* integral identities:

Lemma 26 *Let S be a solution of Eq. (C.1). Then,*

$$\nu ||S||_2^2 + ||S_x||_2^2 - \frac{1}{1+m(0)} ||[1+m(Nx)]^{\frac{1}{p+1}} S||_{p+1}^{p+1} = 0, \tag{C.9}$$

$$-\frac{\nu}{2}||S||_2^2 + \frac{1}{2}||S_x||_2^2 + \frac{||(xm_x)^{\frac{1}{p+1}} S||_{p+1}^{p+1}}{[1+m(0)](p+1)} + \frac{||[1+m(Nx)]^{\frac{1}{p+1}} S||_{p+1}^{p+1}}{[1+m(0)](p+1)} = 0. \tag{C.10}$$

Proof: Multiplying (C.1) by S and integrating gives (C.9). Multiplying (C.1) by $(x \cdot \partial_x S)$ and integrating gives

$$\int (x\ S_x)\Big(-S_{xx} + \nu S - \frac{1+m(Nx)}{1+m(0)}S^p\Big) =$$

$$\int (x\ S_x)_x S_x + \frac{\nu}{2}\int x(S^2)_x + \frac{1}{[1+m(0)](p+1)}\int S^{p+1}\Big([1+m(Nx)]x\Big)_x =$$

$$\int (S_x)^2 + \int (x\partial_x)\frac{(S_x)^2}{2} - \frac{\nu}{2}\int S^2 + \frac{1}{[1+m(0)](p+1)}\int S^{p+1}xm_x$$

$$+\frac{1}{[1+m(0)](p+1)}\int S^{p+1}[1+m(Nx)],$$

from which Eq. (C.10) follows after some algebra. $\square$.

Multiplying (C.9) by $\frac{1}{2}$ and subtracting it from (C.10) gives

$$-\nu\int S^2 + \frac{p+3}{2[1+m(0)](p+1)}\int [1+m(Nx)]S^{p+1} + \frac{\int (xm_x)S^{p+1}}{[1+m(0)](p+1)} = 0.$$

Substituting ansatz (C.3) for S and separating powers of N gives

$$-2\nu\int \mathcal{U}g + \frac{p+3}{2(p+1)}\int \Big(a\ x^2\mathcal{U}^{p+1} + (p+1)\mathcal{U}^p g\Big) + \frac{2a}{p+1}\int x^2\mathcal{U}^{p+1}$$

$$= 0, \tag{C.11}$$

and

$$-2\nu\int \mathcal{U}h - \nu\int g^2 + \frac{1}{p+1}\int 2a(p+1)x^2\mathcal{U}^p g + 4bx^4\mathcal{U}^{p+1}$$

$$+\frac{p+3}{2(p+1)}\int \Big[(p+1)\mathcal{U}^p h + \binom{p+1}{2}\mathcal{U}^{p-1}g^2 + a\ x^2(p+1)\mathcal{U}^p g + bx^4\mathcal{U}^{p+1}\Big]$$

$$= 0. \tag{C.12}$$

Subtracting (C.5) from (C.7) gives $-(p-1)\int \mathcal{U}^p g = a\int x^2\mathcal{U}^{p+1}$. Substituting into (C.11) gives

$$-2\nu\int \mathcal{U}g + a\Big(\frac{p+3}{2(p+1)} + \frac{2}{p+1}\Big)\int x^2\mathcal{U}^{p+1} + \frac{p+3}{2(p+1)}(p+1)\Big(-\frac{a}{p-1}\int x^2\mathcal{U}^{p+1}\Big)$$

$$= -2\nu\int \mathcal{U}g + a\Big(\frac{p+3}{2(p+1)} + \frac{2}{p+1} - \frac{p+3}{2(p+1)}\frac{p+1}{p-1}\Big)\int x^2\mathcal{U}^{p+1},$$

so that

$$2\nu \int \mathcal{U}g = a\frac{p-5}{p^2-1} \int x^2 \mathcal{U}^{p+1}. \tag{C.13}$$

Reorganizing Eq. (C.12)

$$-\nu\left(2\int \mathcal{U}h + \int g^2\right) + \frac{p+3}{2}\int \mathcal{U}^p h + \frac{p(p+3)}{4}\int \mathcal{U}^{p-1}g^2 + a\frac{p+3}{2}\int x^2 \mathcal{U}^p g$$
$$+b\frac{p+3}{2(p+1)}\int x^4\mathcal{U}^4 + 2a\int x^2\mathcal{U}^p g + b\int x^4\mathcal{U}^4$$
$$= \nu\left(-2\int \mathcal{U}h - \int g^2\right) + \frac{p+3}{2}\int \mathcal{U}^p h + \frac{p(p+3)}{4}\int \mathcal{U}^{p-1}g^2 + a\frac{p+7}{4}\int x^2\mathcal{U}^p g$$
$$+b\frac{3p+5}{2(p+1)}\int x^4\mathcal{U}^{p+1} = 0. \tag{C.14}$$

Subtracting (C.6) from (C.8) gives

$$-(p-1)\int \mathcal{U}^p\, h - \frac{p(p-1)}{2}\int \mathcal{U}^{p-1}g^2 = a\,p\,\int x^2\mathcal{U}^p g + b\,\int x^4\mathcal{U}^{p+1}.$$

Multiplying by $-\frac{p+3}{2(p-1)}$ and substituting into (C.14) gives after some algebra

$$\nu\left(2\int \mathcal{U}h + \int g^2\right) = a\,\frac{6p-14}{4(p-1)}\int x^2\mathcal{U}^p g + b\,\frac{p^2-p-4}{(p+1)(p-1)}\int x^4\mathcal{U}^{p+1}. \tag{C.15}$$

Therefore, combining

$$\int S^2 = \int \mathcal{U}^2 + 2N^2\int \mathcal{U}g + N^4\left[2\int \mathcal{U}h + \int g^2\right] + \mathcal{O}(N^6),$$

with (C.13) and (C.15) gives

$$[1+m(0)]^{\frac{2}{p-1}}\int\left[u^{(N)}\right]^2 = \int S^2 = \int \mathcal{U}^2 + N^2\,\frac{a}{\nu}\frac{p-5}{p^2-1}\int x^2\mathcal{U}^{p+1}$$
$$+N^4\left[\frac{a}{\nu}\frac{6p-14}{4(p-1)}\int x^2\mathcal{U}^p g + \frac{b}{\nu}\frac{p^2-p-4}{(p+1)(p-1)}\int x^4\mathcal{U}^{p+1}\right]$$
$$+\mathcal{O}(N^6). \tag{C.16}$$

Therefore, when $p \neq 5$

$$\|u^{(N)}\|_2^2 = [1 + m(0)]^{-\frac{2}{p-1}} \left(\|\mathcal{U}\|_2^2 + N^2 \frac{a}{\nu} \frac{p-5}{p^2-1} \int x^2 \mathcal{U}^{p+1} \right) + \mathcal{O}(N^4).$$

(C.17)

When $p = 5$, the $\mathcal{O}(N^2)$ term vanishes so by Eq. (C.16) and (C.4), the $\mathcal{O}(N^4)$ correction is

$$\|u^{(N)}\|_2^2 =$$
$$= [1 + m(0)]^{-\frac{1}{2}} \left(\|\mathcal{U}\|_2^2 + N^4 \left[\frac{a^2}{\nu} \int x^2 \mathcal{U}^5 L_+^{-1}[x^2 \mathcal{U}^5] + \frac{2}{3} \frac{b}{\nu} \int x^4 \mathcal{U}^6 \right] \right) + \mathcal{O}(N^6)$$
$$= \frac{\|\mathcal{U}\|_2^2}{[1 + m(0)]^{\frac{1}{2}}}$$
$$+ N^4 \frac{18[m''(0)]^2 \int x^2 \mathcal{U}^5 L_+^{-1}[x^2 \mathcal{U}^5] + m^{(4)}(0)[1 + m(0)] \int x^4 \mathcal{U}^6}{72\nu[1 + m(0)]^{\frac{5}{2}}} + \mathcal{O}(N^6)$$
$$= \frac{\|\mathcal{U}\|_2^2}{[1 + m(0)]^{\frac{1}{2}}} - \frac{N^4}{\nu} \frac{\int x^4 \mathcal{U}^6}{72[1 + m(0)]^{\frac{5}{2}}} \left[[m''(0)]^2 G_5 - m^{(4)}(0)[1 + m(0)] \right]$$
$$+ \mathcal{O}(N^6).$$

(C.18)

where $G_5 = -18 \frac{\int x^2 \mathcal{U}^5 L_+^{-1}[x^2 \mathcal{U}^5]}{\int x^4 \mathcal{U}^6} \cong -0.3531$.

Remark 27 *In [21], Fibich and Wang derived relation (C.18) for the critical case for arbitrary dimension. However, the expression that appears in [21] (Eq. (1.12)) has a typographical error. The correct expression is*

$$\|\phi_\omega\|_2^2 = \frac{1}{V^{\frac{d}{2}}(0)} \left[\|R\|_2^2 - \hat{\epsilon}^4 \frac{d \int r^4 R^{4/d+2}}{24(d+2)V^2(0)} \left[[V''(0)]^2 G_d - V^{(4)}(0)V(0) \right] + \mathcal{O}(\hat{\epsilon}^6) \right].$$

(C.19)

D   Perturbation analysis of $\lambda_0^{(N)}$ for $N \ll 1$

In this Appendix we solve the eigenvalue problem (4.10) for $N \ll 1$ and show that it leads to Eq. (4.11). Let

$$f_0^{(N)} = f_0^{(0)}(x) + N^2 f_0^{(2)}(x) + \mathcal{O}(N^4),$$ (D.1)
$$\lambda_0^{(N)} = N^2 \lambda_2 + N^4 \lambda_4 + \mathcal{O}(N^6).$$ (D.2)

By appendix C, $L_+^{(N)}$, defined in (4.1) is

$$L_+^{(N)} = -\partial_x^2 + \nu - p\left(1 + m(0) + N^2 x^2 \frac{m''(0)}{2}\right) \frac{\left(\mathcal{U} + N^2 \frac{m''(0)}{2} L_+^{-1}(x^2 \mathcal{U}^p)\right)^{p-1}}{[1 + m(0)]}$$

$$+ \mathcal{O}(N^4).$$

Hence, the leading order of the eigenvalue problem (4.10) is

$$-\partial_x^2 f_0^{(0)} + \nu f_0^{(0)} - p\mathcal{U}^{p-1} f_0^{(0)} = 0,$$

where $\mathcal{U}$ is given by Eq. (2.10). By Eq. (3.21) we get that $f_0^{(0)}(x) = \mathcal{U}_x$ which is the eigenfunction of the zero eigenvalue, λ_0. The next order is

$$-\partial_x^2 f_0^{(2)} + \nu f_0^{(2)} - p\mathcal{U}^{p-1} f_0^{(2)} = L_+ f_0^{(2)} = \lambda_2 \mathcal{U}_x + \tag{D.3}$$

$$+ p\left(\frac{m''(0)}{2[1 + m(0)]}\right) x^2 \mathcal{U}^{p-1} \mathcal{U}_x + p\left(\frac{m''(0)}{2[1 + m(0)]}\right)\left(L_+^{-1}[x^2 \mathcal{U}^p]\right)(p-1)\mathcal{U}^{p-2}\mathcal{U}_x.$$

Solvability of Eq. (D.3) is ensured by requiring that the right-hand-side of Eq. (D.3) is perpendicular to the null space of L_+ which is spanned by $\mathcal{U}_x$. Therefore,

$$\lambda_2 \int \mathcal{U}_x^2 + p\frac{m''(0)}{2[1 + m(0)]} \int x^2 \mathcal{U}^{p-1} \mathcal{U}_x^2 + p(p-1)\frac{m''(0)}{2[1 + m(0)]} \int \left(L_+^{-1}[x^2 \mathcal{U}^p]\right)\mathcal{U}^{p-2}\mathcal{U}_x^2 = 0.$$

Eliminating λ_2 and using Lemma 28 we get that

$$\lambda_2 \int \mathcal{U}_x^2 = -p\frac{m''(0)}{2[1 + m(0)]} \int x^2 \mathcal{U}^{p-1} \mathcal{U}_x^2 - \frac{m''(0)}{2[1 + m(0)]} \int x^2 \mathcal{U}^p(\mathcal{U} - \mathcal{U}^p) = 0.$$

Using

$$\mathcal{U}_x = -\mathcal{U}\tanh(\frac{p-1}{2}x), \quad \tanh^2(\frac{p-1}{2}x) = 1 - sech^2(\frac{p-1}{2}x) = 1 - \frac{2}{p+1}\mathcal{U}^{p-1}, \tag{D.4}$$

we get that

$$\lambda_2 \int \mathcal{U}_x^2 = -\frac{m''(0)}{2[1 + m(0)]}\left(p\int x^2 \mathcal{U}^{p-1}\mathcal{U}^2(1 - \frac{2}{p+1}\mathcal{U}^{p-1}) - \int x^2(\mathcal{U}^{p+1} - \mathcal{U}^{2p})\right) =$$

$$= -\frac{m''(0)}{2[1 + m(0)]}\int x^2\left(p\mathcal{U}^{p+1} - \frac{2p}{p+1}\mathcal{U}^{2p} - \mathcal{U}^{p+1} + \mathcal{U}^{2p}\right) =$$

$$= -\frac{m''(0)}{2[1 + m(0)]}\int x^2\left((p-1)\mathcal{U}^{p+1} + (1 - \frac{2p}{p+1})\mathcal{U}^{2p}\right) =$$

$$= -(p-1)\frac{m''(0)}{2[1 + m(0)]}\int x^2\left(\mathcal{U}^{p+1} - \frac{1}{p+1}\mathcal{U}^{2p}\right).$$

Numerical evaluation of $\int x^2 \left(\mathcal{U}^{p+1} - \frac{1}{p+1}\mathcal{U}^{2p} \right) > 0$ shows that it is positive for all $p > 1$ (see Fig. D.1). Thus, Eq. (4.11) follows immediately.
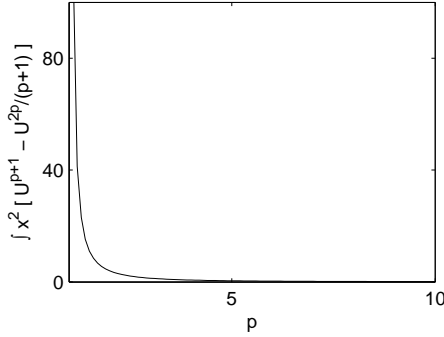

Fig. D.1. Numerical evaluation of $\int x^2 \left(\mathcal{U}^{p+1} - \frac{1}{p+1}\mathcal{U}^{2p} \right)$ as a function of p.

E   Multiple scales expansion of $\lambda_0^{(N)}$ for $N \gg 1$

The eigenvalue problem (4.10) for $\lambda_0^{(N)}$, the analytical continuation of $\lambda_0 = 0$ is

$$\left[-d_x^2 + \nu - p(1 + m(Nx))u^{(N)\,p-1}(x,\nu) \right] f^{(N)}(x;\nu) = \lambda_0^{(N)} f^{(N)}. \qquad (\text{E.1})$$

In the case of wide beams, by Theorem 3, $u^{(N)} = \mathcal{U}(x,\nu) - \frac{1}{N^2}[\partial_X^{-2} m(X)]\mathcal{U}^p + \frac{p\tau_m}{N^2}L_+^{-1}[\mathcal{U}^{2p-1}] + \mathcal{O}(N^{-4})$. Since the solution $f^{(N)}$ is a function of a slow scale x and a fast scale $X = Nx$, we can expand $f^{(N)}$ and $\lambda_0^{(N)}$ in a series of powers of N^{-1} so that

$$
\begin{aligned}
f^{(N)}(x,X) &= f_0(x,X) + \frac{1}{N}f_1(x,X) + \frac{1}{N^2}f_2(x,X) + \cdots, \\
\lambda_0^{(N)} &= \frac{\lambda_1}{N} + \frac{\lambda_2}{N^2} + \cdots.
\end{aligned}
$$

As in Section 3.1, we replace $d_x \to \partial_x + N\partial_X$ so that Eq. (E.1) can be rewritten as

$$\left[-\left(\partial_x^2 + 2N\partial_x\partial_X + N^2\partial_X^2 \right) - p(1+m)(u^{(N)})^{p-1} + \nu \right] f^{(N)} = \lambda_0^{(N)} f^{(N)}. \tag{E.2}$$

Substituting the expansion for $f^{(N)}$ into (E.2) and equating powers of N yields the following hierarchy of equations:

$$\mathcal{O}(N^2) \quad : \quad -\partial_X^2 f_0 \;=\; 0, \tag{E.3}$$

$$\mathcal{O}(N) \quad : \quad -\partial_X^2 f_1 \;=\; 2\partial_X\partial_x f_0, \tag{E.4}$$

$$\mathcal{O}(N^0) \quad : \quad -\partial_X^2 f_2 \;=\; 2\partial_X\partial_x f_1 \;+\; \partial_x^2 f_0 + (1+m)p\mathcal{U}^{p-1}f_0 - \nu f_0, \tag{E.5}$$

$$\mathcal{O}(N^{-1}) : \quad -\partial_X^2 f_3 \;=\; 2\partial_X\partial_x f_2 \;+\; \partial_x^2 f_1 + (1+m)p\mathcal{U}^{p-1}f_1 - \nu f_1 + \lambda_1 f_0, \tag{E.6}$$

$$\mathcal{O}(N^{-2}) : \quad -\partial_X^2 f_4 \;=\; 2\partial_X\partial_x f_3 \;+\; \partial_x^2 f_2 + (1+m)p\mathcal{U}^{p-1}f_2 - \nu f_2 + \lambda_1 f_1$$
$$+\lambda_2 f_0 - (1+m)p(p-1)\mathcal{U}^{p-2}\Big([\partial_X^{-2}\,m]\mathcal{U}^p - p\tau_m L_+^{-1}\mathcal{U}^{2p-1}\Big)f_0, \tag{E.7}$$

where τ_m was defined in Eq. (3.2). We proceed by requiring that f_j are periodic in X. Since the right-hand-side of Eq. (E.3) is zero, by Remark 5, its solution is $f_0 = f_{0,h}(x)$. Consequently, the solution of Eq. (E.4) is $f_1 = f_{1,h}(x)$. Solvability of (E.5) is ensured by setting the average of the right-hand-side of (E.5) equal to zero. This yields

$$L_+ f_{0,h} = 0,$$

so that $f_0 = f_{0,h} = \mathcal{U}_x(x,\nu)$. Therefore, $f_2(x,X)$ satisfies the simplified equation $-\partial_X^2 f_2 \;=\; m(X)\,p\,\mathcal{U}^{p-1}\mathcal{U}_x$ whose solution is

$$f_2 \;=\; -p[\partial_X^{-2}m]\mathcal{U}^{p-1}\mathcal{U}_x \;+\; f_{2h}(x) = \; -[\partial_X^{-2}m]\partial_x(\mathcal{U}^p) + \; f_{2,h}(x).$$

Solvability of (E.6) is ensured by setting the $X-$ average of its right-hand-side equal to zero. This yields

$$-L_+ f_{1,h} = \; \lambda_1 f_{0,h} = \; \lambda_1 \mathcal{U}_x.$$

Hence, for the right-hand-side to be perpendicular to the null space of L_+, $\lambda_1 = 0$ and $f_{1,h} = \mathcal{U}_x$.

Solvability of (E.7) is ensured by setting the $X-$ average of its right-hand-side equal to zero. Calculating the averages term by term gives

$$\langle \partial_x^2 f_2 \; - \nu f_2 + \lambda_2 \mathcal{U}_x \rangle = \partial_x^2 f_{2,h} \; - \nu f_{2,h} + \lambda_2 \mathcal{U}_x,$$
$$p\mathcal{U}^{p-1}\langle (1+m)f_2 \rangle = p\mathcal{U}^{p-1}\Big\langle (1+m)(f_{2,h}(x) - p[\partial_X^{-2}m]\mathcal{U}^{p-1}\mathcal{U}_x)\Big\rangle$$
$$= p\mathcal{U}^{p-1}\Big(f_{2,h} + \tau_m p\mathcal{U}^{p-1}\mathcal{U}_x\Big),$$
$$-p(p-1)\mathcal{U}^{p-2}\mathcal{U}_x \Big\langle (1+m)\Big([\partial_X^{-2}m]\mathcal{U}^p - p\tau_m L_+^{-1}\mathcal{U}^{2p-1}\Big)\Big\rangle$$
$$= -p(p-1)\mathcal{U}^{p-2}\mathcal{U}_x(-\tau_m\mathcal{U}^p + p\tau_m L_+^{-1}\mathcal{U}^{2p-1}).$$

Combining all the above gives

$$L_+ f_{2,h} = p\mathcal{U}^{p-1}\left(\tau_m p\mathcal{U}^{p-1}\mathcal{U}_x\right) - p(p-1)\mathcal{U}^{p-2}\mathcal{U}_x(-\tau_m\mathcal{U}^p + p\tau_m L_+^{-1}[\mathcal{U}^{2p-1}]) + \lambda_2\mathcal{U}_x$$
$$= p^2\tau_m\,\mathcal{U}^{2p-2}\mathcal{U}_x + p(p-1)\tau_m\mathcal{U}^{2p-2}\mathcal{U}_x + p^2(p-1)\mathcal{U}^{p-2}\mathcal{U}_x\tau_m L_+^{-1}[\mathcal{U}^{2p-1}] + \lambda_2\mathcal{U}_x$$
$$= p(2p-1)\tau_m\mathcal{U}^{2p-2}\mathcal{U}_x + p^2(p-1)\mathcal{U}^{p-2}\mathcal{U}_x\tau_m L_+^{-1}[\mathcal{U}^{2p-1}] + \lambda_2\mathcal{U}_x. \qquad \text{(E.8)}$$

Solvability is ensured only if the right-hand-side of Eq. (E.8) is perpendicular to the null space of L_+. Eliminating λ_2 gives

$$\lambda_2 = -p\tau_m\frac{\int \mathcal{U}_x^2\mathcal{U}^{p-2}[p(p-1)L_+^{-1}[\mathcal{U}^{2p-1}] + (2p-1)\mathcal{U}^p]}{\int \mathcal{U}_x^2}. \qquad \text{(E.9)}$$

In order to proceed we use the following Lemma:

Lemma 28 *Let $\mathcal{U}$ be given by (2.10) and let $L_+ = -d_x^2 + \nu - p\mathcal{U}^{p-1}(x,\nu)$. Then, $p(p-1)\mathcal{U}^{p-2}\mathcal{U}_x^2 = L_+\mathcal{U} - L_+\mathcal{U}^p$.*

Proof: Apply L_+ on $\mathcal{U}$ and on $\mathcal{U}^p$. Then eliminate $p(p-1)\mathcal{U}^{p-2}\mathcal{U}_x^2$. $\square$

Substituting for the first term on the right-hand-side of (E.9) and using the fact the L_+ is self adjoint gives

$$\lambda_2 = -p\tau_m\frac{\int \mathcal{U}^{2p} - \mathcal{U}^{3p-1} + (2p-1)\mathcal{U}_x^2\mathcal{U}^{2p-2}}{\int \mathcal{U}_x^2}.$$

Using relations (D.4) gives

$$\lambda_2 = -p\tau_m\frac{\int 2p\mathcal{U}^{2p} - \frac{5p-1}{p+1}\mathcal{U}^{3p-1}}{\int \mathcal{U}_x^2} = -p\tau_m\frac{\int \mathcal{U}^{2p}\left[2p - \frac{5p-1}{p+1}\mathcal{U}^{p-1}\right]}{\int \mathcal{U}_x^2} = 0, \qquad \text{(E.10)}$$

where the integral was evaluated analytically (using Maple) for $p = 3, 5$ and numerically for other values of p. Thus we conclude that $\lambda_0^{(N)} = o(N^{-2})$.

F   Proof of Corollary 24

¿From Eq. (4.18) it follows that the acceleration of the center of mass of the initial condition $\phi_0 = u^{(N)}(x - \delta_c)$ is given by

$$\frac{d^2\,\langle x\rangle}{dz^2}\bigg|_{z=0} = \frac{4N}{p+1}\frac{1}{\int |\phi_0|^2}A(\delta_c),$$

where

$$A(\delta_c) \equiv \int m'(Nx) \; u^{(N)^{p+1}}(x - \delta_c) \; dx = \int m'(N(y + \delta_c)) \; u^{(N)^{p+1}}(y) \; dy.$$

Therefore,

$$A(\delta_c) \cong A(0) + \delta_c \frac{d}{d\delta_c} A(\delta_c)\Big|_{\delta_c=0} = \delta_c N \int m''(Nx) u^{(N)^{p+1}}(x) \; dx.$$

If the width of the input beam is much smaller than the microstructure period $(N \ll 1)$, then, m'' can be replaced with its value at $x = 0$. Hence,

$$sign(A(\delta)) = sign(\delta_c \cdot m''(0)). \tag{F.1}$$

Therefore, a beam close to a local minimum of the microstructure $(m''(0) > 0)$ will accelerate away from it (i.e., towards the nearest maximum) and a beam close to a local maximum of the microstructure $(m''(0) < 0)$ will move towards it.

References

[1] F.Kh. Abdullaev and M. Salerno. Adiabatic compression of soliton matter waves. *J. Phys. B*, 36:2851–2859, 2003.

[2] M.J. Ablowitz and G. Biondini. Multiscale pulse dynamics in communication systems with strong dispersion management. *Opt. Lett.*, 23:1668–1670, 1998.

[3] M.J. Ablowitz, K. Julien, Z.H. Musslimani, and M.I. Weinstein. Wave dynamics in optically modulated waveguide arrays. *Phys. Rev. E*, 71:55602–1–4, 2005.

[4] M.J. Ablowitz and Z.H. Musslimani. Discrete spatial solitons in a diffraction-managed nonlinear waveguide array: a unified approach. *Physica D*, 184:276–303, 2003.

[5] M.J. Ablowitz and Z.H. Musslimani. Spectral renormalization method for computing self-localized solutions to nonlinear systems. *Opt. Lett.*, 30:1–3, 2005.

[6] M.J. Ablowitz, Z.H. Musslimani, and G. Biondini. Methods for discrete solitons in nonlinear lattices. *Phys. Rev. E.*, 65:026602, 2002.

[7] A.B. Aceves. Optical gap solitons: past, present and future; theory and experiments. *Chaos*, 10:584–589, 2000.

[8] A.B. Aceves, G.G. Luther, C. De Angelis, A.M. Rubenchik, and S.K. Turitsyn. Energy localization in nonlinear fiber arrays: collapse-effect compressor. *Phys. Rev. Lett.*, 75:73–6, 1995.

[9] G. Bartal, O. Cohen, T. Schwartz, O. Manela, B. Freedman, M. Segev, H. Buljan, and N.K. Efremidis. Spatial photonics in nonlinear waveguide arrays. *Opt. Exp.*, 13:1780–1796, 2005.

[10] T.B. Benjamin. The stability of solitary waves. *Proc. Roy. Soc. Lond. A*, 328:153–183, 1972.

[11] A. Bensoussan, J.L. Lions, and G.C. Papanicolaou. *Asymptotic Analysis of Periodic Structures*. North Holland, Amsterdam, 1978.

[12] L. Berge, V.K. Mezentsev, J.J. Rasmussen, P.L. Christiansen, and Y.B. Gaididei. Self-guiding light in layered nonlinear media. *Opt. Lett.*, 25:1037–1039, 2000.

[13] F. S. Cataliotti, S. Burger, C. Fort, P. Maddaloni, F. Minardi, A. Trombettoni, A. Smerzi, and M. Inguscio. Josephson junction arrays with Bose-Einstein condenstaes. *Science*, 293:843–6, 2001.

[14] D.N. Christodoulides and R.I. Joseph. Discrete self-focusing in nonlinear arrays of coupled waveguides. *Opt. Lett.*, 13:794–796, 1988.

[15] D.N. Christodoulides and R.I. Joseph. Slow light solitons in nonlinear periodic structures. *Opt. Lett.*, 62:1746–9, 1989.

[16] E.A. Coddington and N. Levinson. *Theory of Ordinary Differential Equations.* McGraw Hill, New York, Toronto, London, 1955.

[17] C.M. de Sterke and J.E. Sipe. Envelope-function approach for the electrodynamics of nonlinear periodic structures. *Phys. Rev. A*, 38:5149–65, 1988.

[18] N.K. Efremidis and D.N. Christodoulides. Lattice solitons in Bose-Einstein condensates. *Phys. Rev. A*, 67:063608, 2003.

[19] H.B. Eisenberg, Y. Silberberg, R. Morandotti, A.R. Boyd, and J.S. Aitchison. Discrete spatial optical solitons in waveguide arrays. *Phys. Rev. Lett.*, 81:3383–3386, 1998.

[20] P.O. Fedichev, Yu. Kagan, G.V. Shlyapnikov, and J.T.M. Walraven. Influence of nearly resonant light on the scattering length in low-temperature atomic gases. *Phys. Rev. Lett.*, 77:2913–6, 1996.

[21] G. Fibich and X.P. Wang. Stability of solitary waves for nonlinear schrödinger equations with inhomogeneous nonlinearities. *Physica D*, 175:96–108, 2003.

[22] J.W. Fleischer, M. Segev, N.K. Efremidis, and D.N. Christodoulides. Observation of two-dimensional discrete solitons in optically-induced nonlinear photonic lattices. *Nature*, page 147, 2003.

[23] V. Fleurov. Discrete quantum brathers: What do we know about them? *Chaos*, 13:676–682, 2003.

[24] A. Floer and A. Weinstein. Nonspreading wave packets for the cubic Schrödinger equation with a bounded potential. *J. Funct. Anal.*, 69:397–408, 1986.

[25] S.E. Golowich and M.I. Weinstein. Scattering resonances of microstructures and homogenization theory. *Multiscale Model. Simul.*, 3:477–521, 2005.

[26] R.H. Goodman, P.J. Holmes, and M.I. Weinstein. Strong NLS soliton-defect interactions. *Physica D*, 192:215–248, 2004.

[27] R.H. Goodman, R.E. Slusher, and M.I. Weinstein. Stopping light on a defect. *J. Opt. Soc. Am. B*, 19:1635–1652, 2002.

[28] M.G. Grillakis. Linearized instability for nonlinear Schrödinger and Klein-Gordon equations. *Comm. Pure Appl. Math.*, 41:747–774, 1988.

[29] M.G. Grillakis, J. Shatah, and W.A. Strauss. Stability theory of solitary waves in the presence of symmetry i. *J. Funct. Anal.*, 74(1):160–197, 1987.

[30] H. Hajaiej and C.A. Stuart. On the variational approach to the stability of standing waves for the nonlinear Schrödinger equation. *Adv. Nonlinear Stud.*, 4:469–501, 2004.

[31] D.C. Hutchings. Theory of ultrafast nonlinear refraction in semiconductor superlattices. *IEEE Journal of selected topics in quantum electronics*, 10:1124–1132, 2004.

[32] J.J. Joannopoulos, R.D. Meade, and J.N. Winn. Photonic crystals - molding the flow of light. *Princeton University Press*, 1995.

[33] C.K.R.T. Jones. An instability mechanism for radially symmetric standing waves of a nonlinear Schrödinger equation. *J. Diff. Equa.*, 71:34–62, 1988.

[34] T. Kapitula. Stability of waves in perturbed hamiltonian systems. *Physica D*, 156:186–200, 2001.

[35] J.P. Keener. Homogenization and propagation in the bistable equation. *Physica D*, 136:1–17, 2000.

[36] D. Mandelik, R. Morandotti, J.S. Aitchison, and Y. Silberberg. Gap solitons in waveguide arrays. *Phys. Rev. Lett.*, 92:093904–093907, 2004.

[37] F. Merle. Asymptotics for L^2 minimal blow-up solutions of critical nonlinear Schrödinger equation. *Ann. Inst. H. Poincaré Anal. non linéaire.*, 13:553–565, 1996.

[38] F. Merle. Nonexistence of minimal blow-up solutions of equations $iu_t = -\Delta u - k(x)|u|^{4/N}u$ in $\mathbf{R}^N$. *Ann. Inst. H. Poincaré Phys. Théor.*, 64:33–85, 1996.

[39] G.D. Montesinos, V.M. Perez-Garcia, and P.J. Torres. Stabilization of solitons of the multidimensional nonlinear Schrödinger equation: matter-wave breathers. *Physica D*, 191:193–210, 2004.

[40] R. Morandotti, U. Peschel, J.S. Aitchison, H.S. Eisenberg, and Y. Silberberg. Dynamics of discrete solitons in optical waveguide arrays. *Phys. Rev. Lett.*, 83:2726–2729, 1999.

[41] Z.H. Musslimani and J. Yang. Self trapping of light in a two dimensional photonic lattice. *J. Opt. Soc. Am. B*, 21:973–981, 2004.

[42] Y.-G. Oh. Stability of semiclassical bound states of nonlinear Schrödinger equations with potentials. *Comm. Math. Phys.*, 121:11–33, 1989.

[43] D.E. Pelinovsky, P.G. Kevrekidis, and D.J. Frantzeskakis. Averaging for solitons with nonlinearity management. *Phys. Rev. Lett.*, 91:240201, 2003.

[44] V.I. Petviashvili. Equation of an extraordinary soliton. *Sov. J. Plasma Phys.*, 2:257, 1976.

[45] M. Reed and B. Simon. *Methods of Modern Mathematical Physics, IV. Analysis of Operators.* Academic Press, New York, 1978.

[46] H.A. Rose and M.I. Weinstein. On the bound states of the nonlinear Schrödinger equation with a linear potential. *Physica D*, 30:207–218, 1988.

[47] H. Sakagouchi and B.A. Malomed. Resonant nonlinearity management for nonlinear Schrödinger solitons. *PRE*, 70:066613, 2004.

[48] H. Sakagouchi and B.A. Malomed. Matter-wave solitons in nonlinear optical lattices. *PRE*, 72:046610, 2005.

[49] A. Smerzi and A. Trombettoni. Discrete nonlinear dynamics of weakly coupled Bose-Einstein condensates. *Chaos*, 13:766–776, 2003.

[50] W.A. Strauss. *Nonlinear Wave Equations*. Amer. Math. Soc., Providence, R.I., 1989.

[51] A.A. Sukhorukov, Y.S. Kivshar, H.B. Eisenberg, and Y. Silberberg. Spatial optical solitons in waveguide arrays. *IEEE J. of Qu. Elec.*, 39:31–50, 2003.

[52] C. Sulem and P.L. Sulem. *The Nonlinear Schrödinger Equation*. Springer, New York, 1999.

[53] G. Theocharis, P. Schmelcher, P.G. Kevrekidis, and D.J. Frantzeskakis. Matter-wave solitons of collisionally inhomogeneous condensates. *Phys. Rev. A*, 72:033614, 2005.

[54] M. I. Weinstein. *in The Connection Between Finite and Infinite-Dimensional Dynamical Systems*. Amer. Math. Soc., Providence, R.I., 1989.

[55] M.I. Weinstein. Nonlinear Schrödinger equations and sharp interpolation estimates. *Comm. Math. Phys.*, 87:567–576, 1982/3.

[56] M.I. Weinstein. Modulational stability of ground states of nonlinear Schrödinger equations. *SIAM J. Math. Anal.*, 16:472–491, 1985.

[57] M.I. Weinstein. Lyapunov stability of ground states of nonlinear dispersive evolution equations. *Comm. Pure Appl. Math.*, 39:51–68, 1986.

[58] M.I. Weinstein. Excitation thresholds for nonlinear localized modes on lattices. *Nonlinearity*, 12:673–691, 1999.

[59] M.I. Weinstein and B. Yeary. Excitation and dynamics of pulses in coupled fiber arrays. *Phys. Lett. A*, 222:157–162, 1996.